2008

EFFECTS OF METAL PROTOPORPHYRINS ON BURN WOUND CONVERSION

Katie Braun
Virginia Commonwealth University

EFFECTS OF METAL PROTOPORPHYRINS ON BURN WOUND CONVERSION

A thesis submitted in partial fulfillment of the requirements for the degree of Master of Science at Virginia Commonwealth University.

by

KATIE LYNNE BRAUN
Bachelor of Science, Health Science, James Madison University, 2006
Master of Science, Physiology, Virginia Commonwealth University, 2008

Director: DORNE R. YAGER, Ph. D.
ASSOCIATE PROFESSOR & DIRECTOR OF RESEARCH
DEPARTMENT OF SURGERY
DIVISION OF PLASTIC SURGERY

Virginia Commonwealth University
Richmond, Virginia
December 8, 2008

Acknowledgment

To begin, I would like to thank Dr. Dorne Yager for the opportunity to work on this project in his lab. He was an amazing advisor and I thoroughly enjoyed spending my time researching under his supervision. He was extremely patient and very dedicated, not only to the project but also to my learning experience. I would also like to thank the other members in the lab Dr. Kunoor Jain, Dr. Carter Tuttle, Dr. David Lanning, and Virginia Sykes, who on many occasions helped me with questions regarding experimental methods or offering instruments and materials when needed. I would like to thank Dr. Vijay Lyall and Dr. Robert Diegelmann for serving on my committee. I would like to thank Dr. Steven Price for his instruction in public speaking and for taking the time to serve on my committee as well. I would like to thank Kim Oh, my lab partner, for the wonderful company every day and the intelligence and support that she portrayed throughout the year. I would like to thank Nicholas Troxel for his kindness and understanding throughout this experience. Lastly, I would like to thank my family. My parents, Ashley, Cecelia, and Dan have all been there for me through everything and I do not know where I would be today without any of them. Their unfailing love, encouragement, and support have given me the motivation to pursue all of my dreams.

Table of Contents

Page

List of Tables

List of Figures

List of Abbreviations

HO	heme oxygenase
HO – 1	heme oxygenase – 1
HO – 2	heme oxygenase - 2
MPO	myeloperoxidase
MMP	matrix metalloproteinase
ATP	adenosine triphosphate
AMP	adenosine monophosphate
Co PP	cobalt protoporphyrin
Sn PP	stannous protoporphyrin
ROS	reactive oxygen species
EPO	erythropoietin
CrMP	chromatin mesoporphyrin
I.P.	intraperitoneally
PBS	phosphate buffered saline
BSA	bovine serum albumin
HClO	hypochlorous acid
HTAB	hexadecyltrimethyl -ammonium bromide
PMN	polymorphonuclear leukocyte
TCA	trichloroacetic acid

SDS – PAGE	sodium dodecyl sulfate polyacrylamide gel electrophoresis
DTT	dithiothreitol
BpB	*N*,*N*′-bis(2-pyridinecarboxamide)-1,2-benzene dianion
AP	ammonium persulfate
TEMED	tetramethylethylene - diamine
TBST	Tris-Buffered Saline Tween - 20
PVDF	polyvinylidene fluoride
APMA	aminophenylmercuric acetate
EDTA	ethylenediamene tetraacedic acid
s.c.	sub-cutaneously
CO	carbon monoxide

Abstract

EFFECTS OF METAL PROTOPORPHYRINS ON BURN WOUND CONVERSION

By Katie Lynne Braun, M.S.

A thesis submitted in partial fulfillment of the requirements for the degree of Master of Science at Virginia Commonwealth University.

Virginia Commonwealth University, 2008

Major Director: Dorne R. Yager, Ph. D.
Associate Professor & Director of Research, Department of Surgery

A murine model was utilized to test the influence of heavy metal protoporphyrins on burn conversion, heme oxygenase – 1 (HO-1) expression, and inflammation. Heavy metal protoporphyrins, such as cobalt protoporphyrin (Co PP) and tin protoporphyrin (Sn PP), were used to influence the heme oxygenase activity. The effects of these heavy metal protoporphyrins on burn wound conversion were examined using a burn comb model in rats.

In addition to assessing the extent of conversion, HO-1 expression and parameters of inflammation were also examined in the area of injury (interspace region) subject to conversion. These studies demonstrate proof in principal that pharmacologic

agents known to modify HO activity can also modulate burn wound conversion. Improved outcome correlated with HO-1 expression/activity and reduced inflammation. This suggests that one of the mechanisms utilized by HO-1 to improve burn wound outcome involves modulation of one or more components of the inflammatory response.

Introduction

General Purpose

In the United States, approximately two million people each year are subject to burn injury. Of these, 80,000 require hospitalization, and 6,500 die as a direct or indirect result of their burn injuries. (Singh, Devgan et al., 2007) Burns and their recorded treatment date back to the 15th century B.C. In the Ebers papyrus, burn wounds were treated with "cattle dung and black mud" (Weeks & Xu, 2004). It was not until the twentieth century that significant progress in the treatment of burn wounds occurred. With the First World War, autologous surgical skin grafts came into use and beginning in the 1960s fluid resuscitation techniques greatly reduced mortality resulting from shock. (Weeks & Xu, 2004)

One of the significant problems that are still encountered with burn wounds is conversion. For reasons that are not entirely appreciated, burn wound severity is not always static and can progressively worsen following the initial injury. This is clinically relevant because it not only confounds diagnosis but, burns that progress from partial-thickness to full-thickness injury are at a much greater risk for hypertrophic scarring and contracture. Full-thickness burn wounds also put the individual at increased risk for sepsis and require surgical interventions. Although the mechanisms behind burn wound conversion are incompletely understood, there is a consensus that inflammation plays a major role. (Singh, Devgan et al., 2007)

The stress protein, heme oxygenase-1 (HO-1) generates products with anti-inflammatory functions. The expression and activity of HO-1 can be pharmacologically modulated by heavy metal protoporphyrins. Therefore, the goals of this study were:

1. test whether heavy metal protoporphyrins influence burn conversion
2. test whether protoporphyrins influence HO – 1 expression
3. test whether heavy metal protoporphyrins influence inflammation, using markers such as myeloperoxidase (MPO) and matrix metalloproteinase (MMP) expression

Hypothesis

Experimental analysis will demonstrate that heavy metal protoporphyrins, tin protoporphyrin (Sn PP) and cobalt protoporphyrin (Co PP) will have an effect on the conversion of the burn injury. By testing the key elements in the Co PP and Sn PP treated inflamed tissue, will show that HO-1 expression is increased. Heavy metal protoporphyrins should modulate HO-1 expression. Inflammation and necrosis should correlate with an environment in which HO-1 is inhibited, and should inversely correlate with a pharmacologic regimen that increased HO-1 activity. There is a correlation between Co PP and Sn PP treatments that modulate HO-1 expression/activity with inflammation and necrosis. Co PP and Sn PP should be observed to have a significant influence on the inflammation of the burned tissue and MMP expression.

Background

When skin is heated, it is subject to damage as a result of the transfer of thermal energy. Temperature and duration of exposure are the two most important determinants of the degree of injury. Physics dictates that thermal damage is dependent upon the quantity of heat that is transferred and the extent to which it is dissipated. The last two decades have seen significant advances in burn care. The number of deaths annually in the United States is now less than a third of that seen in 1970. Moreover, the size of burn associated with a 50 percent survival rate has increased from 30% of the total body surface area to well over 80% in otherwise healthy adults. (Warden & Heimbach, 1999)

The skin is composed of layers, all of which can be affected by a burn depending on the severity. The three main layers are the epidermis, dermis, and hypodermis. The epidermis consists of different types of cells: keratinocytes, melanocytes, Merkels cells, and Langerhans cells. Blood vessels can not be found in the epidermis, but oxygen and nutrients reach the tissue by way of diffusion from the dermis. The main function of the epidermis is to act as a protective barrier. The epidermis is divided into five separate layers. Starting from the top, there is the stratum corneum, stratum lucidum, stratum granulosum, stratum spinosum, and the stratum basale, which borders the dermis. The stratum corneum is composed of dead cells or cells that are close to death. This sub-layer of the epidermis acts as a protective surface due to the strength of the keratin protein in the dying cells. Although this layer has many dying cells, hydration is still possible. The stratum lucidum is only apparent in thick skin which helps to decrease

friction. The stratum granulosum contains keratinocytes which produce keratin proteins and lipids responsible for hydration of the epidermis. The stratum spinosum again contains keratinocytes which begin the production of keratin. Langerhans cells are also found in the stratum spinosum and are very important to the epidermis. These cells relay signals to the immune system and help to protect to body from foreign invaders or any other trauma to the skin. The last layer of the epidermis is the stratum basale and its main function is to form new cells that are forced upward as the stratum corneum sloughs off dying cells. The stratum basale contains melanocytes and Merkels cells. Melanocytes produce melanin pigment to help protect the skin from sun damage. Merkels cells do not have a determined function, but could potentially be related to the touch sense. (Brannon, 2007; Gary, 2008; Kenet & Lawyer, 1994)

The dermis is made up of two layers: papillary and reticular layer. The upper level is the papillary dermis and the lower level is the reticular dermis. The whole dermis is formed from connective tissue. Specifically, the papillary layer is composed of thin collagen fibers and the reticular layer is made up of thick collagen fibers, which provide support. There are many more components involved in the dermis. Elastin runs throughout this layer, which provides elasticity to the skin. The dermis also contains hair follicles and erector pili muscles, sweat glands, blood vessels, lymph vessels, and nerves. Meissner's and Pacini corpuscles in the dermis sense touch and pressure. Histiocytes are found in the dermis as well, and serve as important factors involved in the healing process and regeneration of the epidermis. Monocytes derived from the bone marrow become histiocytes when arriving in the dermis in response to trauma.

Overall, the dermis provides elasticity, support, and strength to the skin and begins the process of repair. (Gomez & Cancio, 2007) Therefore, the deeper a burn progresses into the skin, the more severe a burn (Singh, Devgan et al., 2007).

The innermost layer of the skin is the hypodermis. The hypodermis contains much of the fat stored in the body, but also consists of connective tissue, large blood vessels, hair follicle roots, and nerve endings. The adipose cells in this layer act as a shock absorber and provide insulation for the body. (Hettiaratchy & Dziewulski 2004; Benson, Dickson et al., 2006)

The extent of burn wound damage in the layers of the skin is commonly classified in terms of degrees. First degree burns (or superficial burns) are the most minor and do the least amount of damage. These burns will make the skin turn pink or red and only affects the epidermis. An example would be a typical sun burn. Second degree burns (or partial-thickness burns) extend deeper into the skin and involve all or part of the dermis. Second degree burns can be sub-classified as superficial partial-thickness burns (involving the papillary dermis) or deep partial-thickness burns (involving the papillary and reticular dermis). Second degree burns result in blistering of the skin, can be painful depending on the quantity and depth of nerves affected, and result in damage to the epidermis and dermis. Third degree burns involve the epidermis, dermis, and extend into the subcutaneous tissues. Severe burns can involve muscle and bone. (Barton, Kokoska et al., 2006; Gomez & Cancio, 2007) See Figure 1.

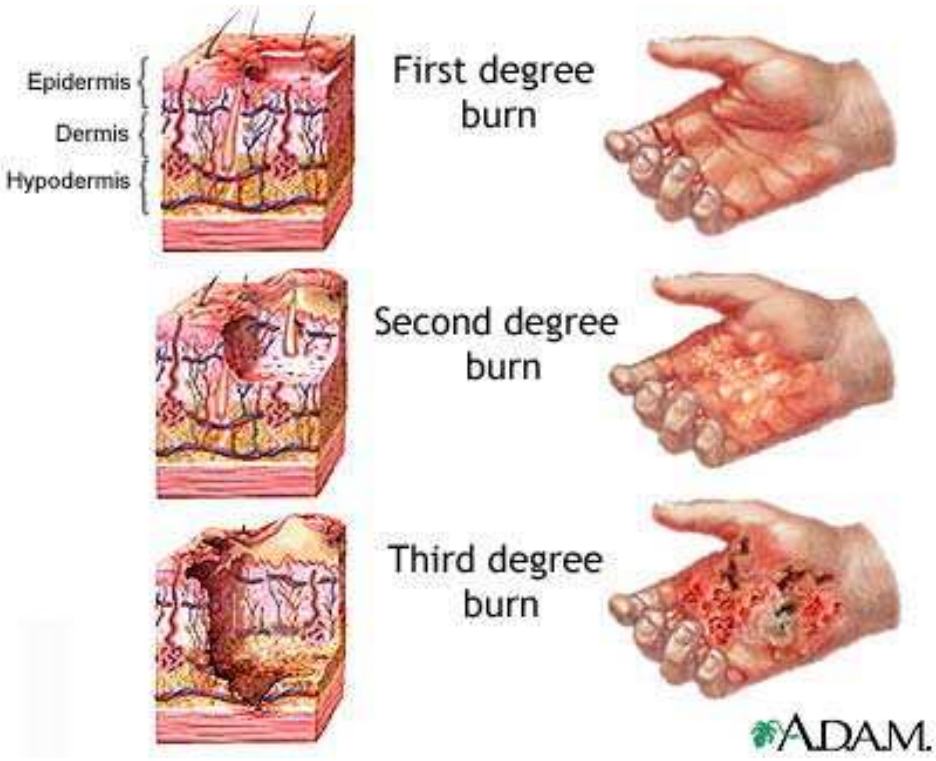

Figure 1: Degree Levels of Burns

In addition, individual burn wounds are also defined in terms of evolving injury. Burn wound conversion is a process in which superficial burns develop into deeper burn wounds. Jackson was the first to determine that a burn can be observed as three separate zones: the zone of coagulation, the zone of stasis, and the zone of hyperemia. See Figure 2. The zone of coagulation refers to the area of injured tissue which has received irreversible damage. The tissue has been destroyed and the cells die extremely quickly. This area is void of any blood flow and damage is irreversible. Deep and peripheral to the zone of coagulation is the zone of stasis. Due to direct thermal effects, the microvasculatures in this region dilate and its endothelial lining 'leaks' plasma and intravascular proteins. With time, the circulation in this region ceases as the capillaries become packed with red blood cells and microthrombi, aggravating the inflammatory response. With appropriate treatment, the cellular damage in this region is potentially reversible. The outermost zone is the zone of hyperemia. Damage in this area is severe, but not permanent. The blood flow increases daily and healing should be apparent after about a week. (Gomez & Cancio, 2007; Singh, Devgan et al., 2007)

"The depth of burn wounds is not entirely static, however, and multiple factors, each acting via a variety of pathophysiologic mechanisms, can promote the deepening of a burn wound. In a subacute time frame of 3–5 days, burns originally assessed to be superficial partial thickness have been observed to progress into deep partial-thickness or full-thickness burns. This process of progressive damage to initially unburned tissue surrounding a burn wound is referred to as burn wound progression, which remains clinically important but poorly understood" (Singh, Devgan et al., 2007).

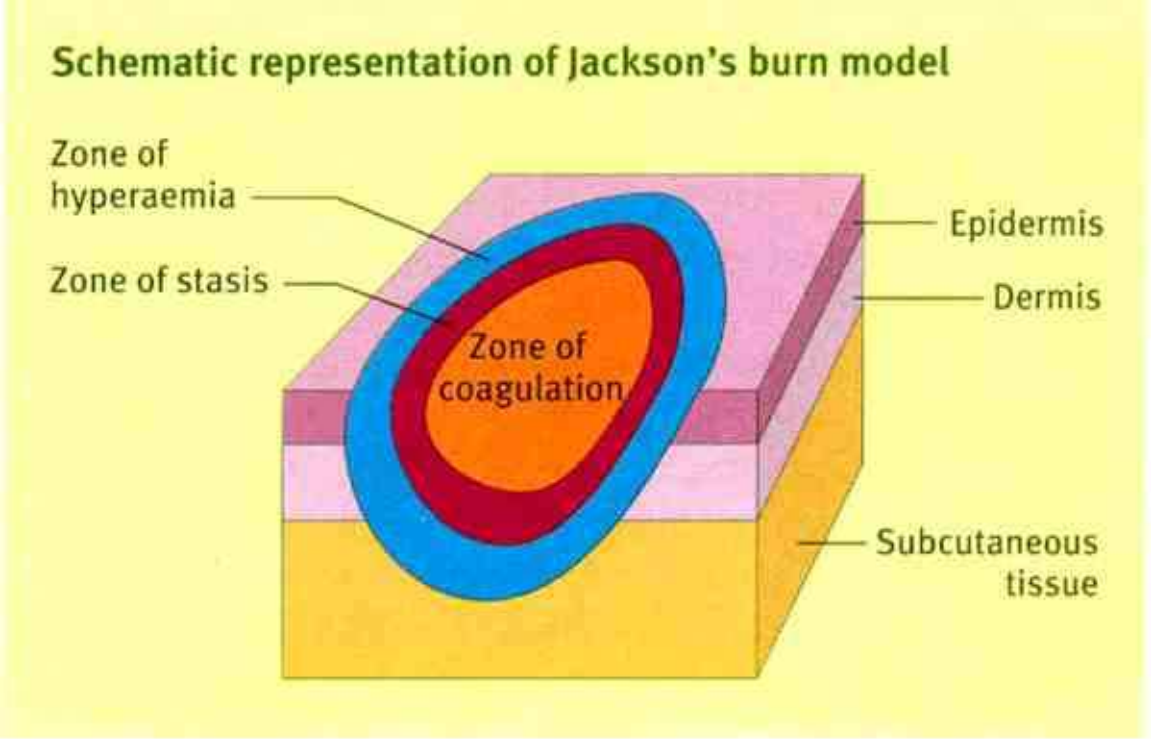

Figure 2: Zones of Stasis in Burn Wound Conversion

A number of systemic and local factors and cellular mechanisms can be involved in burn wound conversion. Local and systemic factors include infection, edema, altered perfusion caused by circumferential eschar, general health (e.g., age), shock, inadequate fluid resuscitation, cytokine alterations, and pathologies such as atherosclerosis, peripheral vessel disease, and diabetes. Edema, decreased fluid resuscitation, and altered perfusion can all cause cell death because of a drop in intravascular and interstitial fluid volumes. The alterations in cytokine levels increase the chances of infection. Diabetes can occur due to decreased metabolic function. General health is very important as well because with a compromised immune system due to age or lifestyle, the ability for the body to heal is reduced. Models that have been used to study factors that affect burn wound conversion have already showed that fluid resuscitation can turn a partial thickness burn into a full thickness burn. (Singh, Devgan et al., 2007)

Molecular mechanisms that have been suggested to contribute to burn wound conversion are diverse but most are directly or indirectly related to inflammation. Prostaglandins are formed through the action of cyclooxygenase. Certain prostaglandins are inhibitors of platelet aggregation and serve to vasodilate, whereas others act as potent vasoconstrictors and promote aggregation of platelets. Alterations in prostanoid levels can lead to vasoconstriction and thus a reduction in perfusion. (Robson, 1979) Conversely, increased levels of nitric oxide and pro-inflammatory cytokines can cause vasodilation resulting in edema and tissue congestion (Rawlingson, 2003).

In 1968, McCord and Fridovich proposed that the enzyme xanthine oxidase was the major source of free radicals that contributed to reperfusion injury. Altered peripheral

perfusion decreases the oxygen available to peripheral tissues that is required for adenosine triphosphate (ATP) production. As ATP depletion occurs, the level of adenosine monophosphate (AMP) rises and, in turn, is catabolized to hypoxanthine. The return of molecular oxygen to previously ischemic tissues results in hypoxanthine serving as a substrate for xanthine oxidase. In a series of complicated reactions, hypoxanthine is converted to xanthine and ultimately to uric acid, and this process produces hydrogen peroxide and superoxide, deleterious oxygen-derived free radicals. (McCord & Fridovich, 1968)

Another major source of reactive oxygen species (ROS) in burn trauma comes from activated neutrophils. Activated neutrophils produce a burst of free radicals (Basadre et al., 1988; Horton et al., 1996; Horton & Garcia, 1995; Mileski et al., 1991). This neutrophil-related function serves a significant protective mechanism by scavenging invading bacteria; however, with injury such as burn trauma, a burst of neutrophil-produced free radicals in addition to xanthine oxidase activity, may result in overwhelming tissue damage. Moreover, while burn trauma increases ROS production, this type of traumatic injury also impairs antioxidant defense mechanisms, rendering the burn subject more susceptible to oxygen free radical mediated injury. For example, numerous studies have shown that burn trauma alters non-enzymatic defense mechanisms including decreases in alpha tocopherol, and ascorbic acid. These endogenous antioxidant mechanisms protect membranes against lipid peroxidation, scavenge oxygen derived free radicals, and dissipate free radical energy. In addition, burn trauma alters enzymatic defense mechanisms including altered superoxide

dismutase levels, reduced catalase and reduced glutathione levels (Cynober et al., 1985; Demling et al., 1995; Demling and LaLonde, 1990a; Demling and LaLonde, 1990b; LaLonde et al., 1992; LaLonde et al., 1997a; LaLonde et al., 1997b; Nguyen et al., 1993; Rai & Courtemanche, 1975; Sasaki et al., 1990).

Recent attention has focused on the hypothesis that the accumulation of reactive biochemical species such as oxygen derived free radicals and non-radicals such as hydrogen peroxide and nitric oxide promote and exacerbate the inflammatory response (Cain et al., 1999; Giroir et a., 1994). Inflammation is a standard immediate response to inury, including burns. Acute inflammation is a natural defense to skin trauma. Non-specific inflammation activates cascades such a complement, prostaglandins, and then the migration of neutrophils. Burn wounds have been observed to produce the non-specific inflammatory response, although it has not been proven. Mediators of the inflammatory response act locally and systemically. Cytokines produced in response to inflammation initiate the leukocyte response. Overproduction of cytokines can lead to a "domino effect" and the inflammatory response can become widespread leading to systemic inflammatory response syndrome, acute respiratory distress syndrome, or multiple organ dysfunction syndrome. Although there are many cell types involved in the inflammatory response, research on animal models has shown that neutrophils and macrophages tend to predominate the injured tissue. (Tyler, Watts et al., 2000; Dokumcu, Ergun et al., 2008)

In addition to their ability to generate ROS, neutrophils possess several types of granules in which are packaged large amounts of degradative enzymes such as serine

proteinases (e.g., elastase and cathepsin G) and matrix metalloproteinases (e.g., MMP-8 and MMP-9). Although these enzymes and the associated respiratory burst are designed to aid in debridement of devitalized tissues and destruction of microbes there is a growing appreciation that an over exuberant response by neutrophils can lead to additional damage of tissues. (Yager & Nwomeh, 1999)

Heme Oxygenase – 1

As outlined in the preceding section, there is evidence that a number of local and molecular factors associated with inflammation are involved in burn wound conversion. Therefore, targeting the inflammatory response could provide a means for modulating conversion. Heme oxygenases are very important in the response to injury by amplifying inflammation (Burger, Xiang et al., 2008). Being able to control heme oxygenase (HO) would be extremely beneficial to decreasing the effects of burn wound conversion.

HO is the first and rate-controlling enzyme of the degradation of heme into iron, carbon monoxide, and biliverdin, the latter being subsequently converted into bilirubin. See Figure 3. Several positive biological effects exerted by this enzyme have gained attention. Heme is a potent oxidant, removal of free heme from the area of a burn injury is likely to be beneficial. Perhaps just as important, carbon monoxide and bilirubin have been attributed to possess anti-inflammatory, antiapoptotic, angiogenic, and cytoprotective functions. (Farombi & Surh, 2006) Experimentation conducted by

Burger studied the effects that HO-1 had on erythropoietin (EPO), which is a hormone that can protect the heart from ischemia and reperfusion. EPO was shown to induce expression of HO-1. Apoptosis was decreased by an increase in expression of HO-1. Burger showed that the "selective inhibition of HO-1 using chromatin mesoporphyrin (CrMP) significantly diminished the ability of erythropoietin to inhibit apoptosis." HO-1 appeared to introduce a protective role in regards to arthrosclerosis and endotoxemia. (Burger, Xiang et al., 2008) Thus, the physiological induction of HO-1 may be an adaptive and beneficial response to several possibly noxious stimuli, including heme itself, suggesting a potentially autoprotective and autodefensive role in burn wound pathology.

There are two genetic isoforms: HO-1 and HO-2. HO-1 expression is inducible in virtually every cell type. In contrast, HO-2 is expressed constitutively in a limited number of tissues amino acids. (Farombi & Surh, 2006) HO – 1 binds to heme in a 1:1 ratio. HO-1 in humans portrays a flexible bihelical structure which encompasses the heme pocket. Expression of HO-1 is apparent in large concentrations in the spleen, liver, and bone marrow. Within cells HO is abundant in the endoplasmic reticulum. Studies have provided some evidence of HO expression in the plasma membrane and the nucleus. (Ryter, Alam et. Al, 2006) Under normal physiological conditions most other tissues express only very low levels of HO-1.

HO-1 synthesis is greatly amplified in response to biological stress of the body and tissues and serves as a protective mechanism in response to many different stimuli. For

example, heat shock, oxidative stress, UV radiation, and hydrogen peroxide are all found to induce the synthesis of HO-1. Although outside stresses can influence the levels of HO-1 produced in the body, injury or infection caused by systemic stress can also bring about the cytoprotectant role of HO-1. HO-1 is strongly activated by a number of proinflammatory agents. Devey studied ischemia reperfusion injury in the liver. HO-1 was observed to have anti-inflammatory actions and protect cells from oxidative injury. When HO-1 was deleted in mice, the animals were susceptible to hepatic ischemia reperfusion (Devey, Ferenbach et al., 2008). Most studies involving HO-1, even though involving different parts of the body, show that HO-1 is probably essential for maintaining cellular homeostasis in the body. Growth retardation, anemia, iron deposition, and vulnerability to stressful injury are all observed in HO-1 knockout. Animals presented as HO-1 knockout normally do not survive. (Poss & Tonegawa, 1997) In addition, a similar phenotype has been observed in the one reported instance of a human with HO-1 deficiency (Yachie, Niida et al., 1999).

Heme oxygenases have become recognized as major protective proteins. Increased expression of HO-1 has been shown to be effective in preventing or ameliorating pathologies associated with atherosclerosis, angioplasty, chronic allograft rejection, inflammatory lung disease, LPS-induced endotoxemia, and ischemia reperfusion injury. Degradation of heme not only reduces the oxidative potential within tissues, but the products generated by the degradation of heme have potent antioxidant, anti-inflammatory, anti-proliferative, and anti-apoptotic properties.

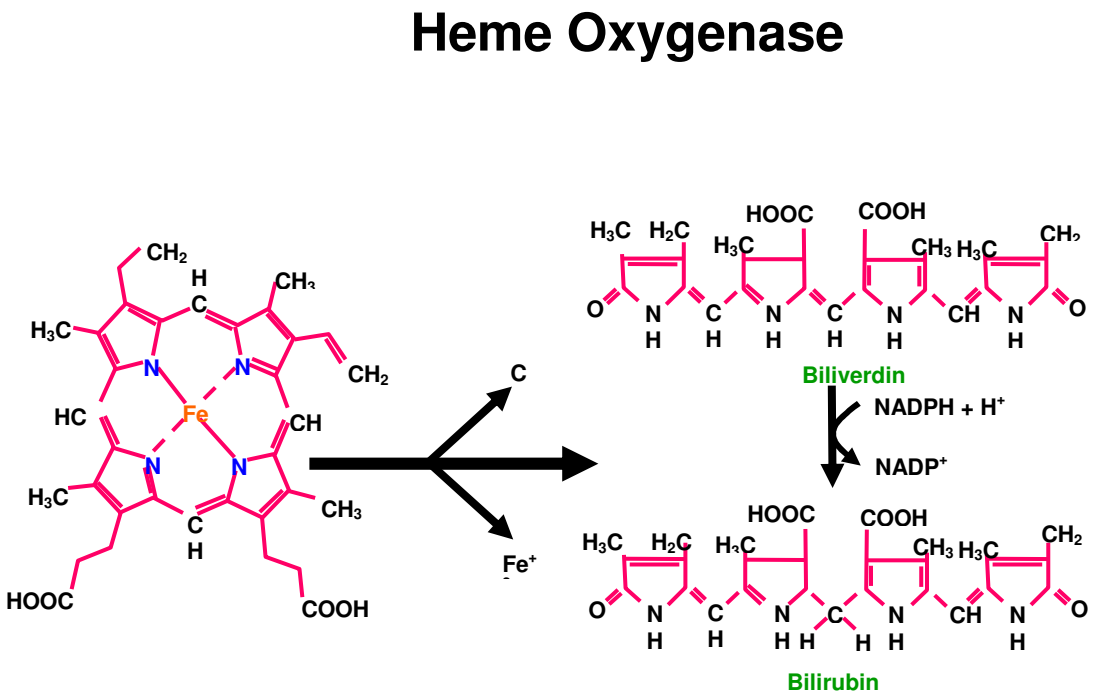

Figure 3: Pathway of heme metabolism.

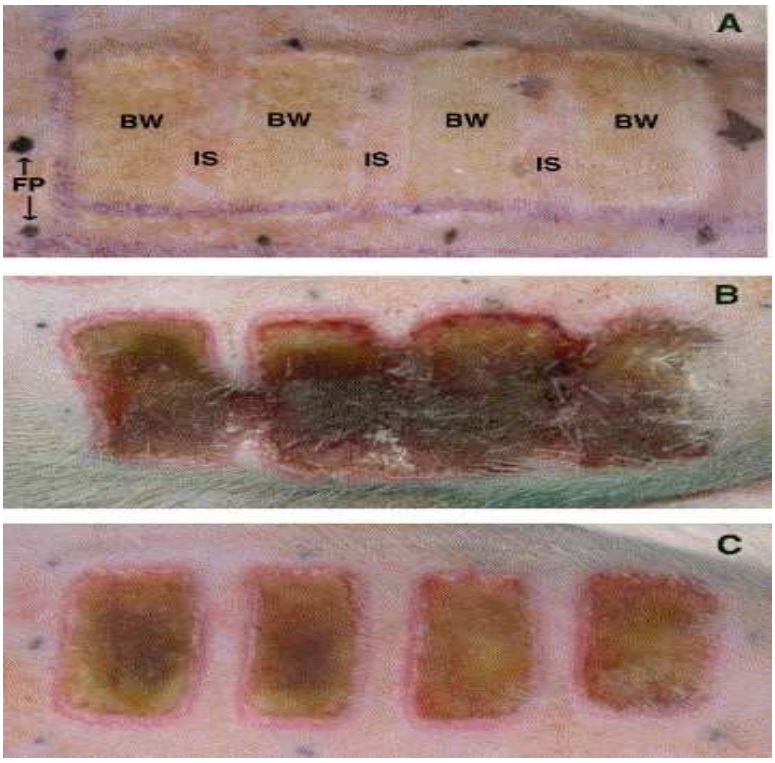

Figure 4: Example of Research Objective:
(A) Immediately post burn: intervening space (IS); burn wound.
(B) Seven days post wounding.
(C) Seven days post wounding with treatment (Mahanjan et al., 2006)
They used 1 x 2 cm burns with 0.5 cm IS. I want to increase the IS to 1 cm.

Methods and Materials

Burn Wound Healing of Animals Protocol

The expression and influence of HO-1 on burn wounds was tested using Wistar male rats (Harlan Sprague Dawley, Inc., Indianapolis, IN). The standard outbred rat weighed approximately 225 g. The animals were delivered to Sanger Hall and allowed to acclimate to the new surroundings for about a week. Twenty four hours prior to the wounding procedure 0.1 cc of 5 mg/kg CoPP or 0.2 cc of 30 μM/kg SnPP were administered to the animal via intraperitoneal (I.P.) injection. The oxygen tank regulator in the surgery room was checked in order to make sure it was full. Polyethylene glycol pads were heated to 39°C.

On the day of the procedure, water was brought to 100°C and a thermometer was used to monitor the temperature. A brass template (brand) specially made to wound the rats was placed in the boiling water. Refer to Figure 4. The template was made with three brass prongs and a wooden handle. The prongs were spaced 0.5 cm apart and each prong was 2 cm in height and 1 cm in length. Refer to Figure 5.

Anesthesia was induced with 4-5% isofluorane at 1.0 Liter/min. Following induction, the animal was removed from the induction chamber and placed in a nose cone that provided 2% isofluorane at 0.5 Liter/min. A toe pinch was administered to ensure the animal was under anesthesia. The tail was marked with a black Sharpie for identification purposes, and 0.2 cc of 125 μg/μL buprenorphine administered

subcutaneously (s.c.) in the skin on the back of the animal above a rear leg. Clippers were used to remove the hair from the upper trunk region of the animal. Chemical depiliation (Nair) was used to remove the remaining hair. Phosphate buffered saline (PBS) pH 5.0 was used to rinse the area and neutralize the chemical depilator. The skin was dried thoroughly.

The brand was taken out of the 100°C water, briefly dried and applied to the skin for 45 seconds using the weight of the brand for pressure. This produced a reproducible full-thickness burn where the brand directly touched the skin. In addition, the two interspace regions frequently also became necrotic. In this model, the interspace region represents a zone of stasis. A labeled ruler tape was placed beneath the wound and a photograph was taken to document the brand. The animal was then placed in the recovery chamber for about 10-15 minutes or until walking around and alert, and then placed in appropriate cages. The procedure was documented on the data sheets. As follow up, the branded animals were given 0.2cc of 125 µg/mL buprenorphine twice a day for two days and then on days 3-7 (or until sacrificed) provided one “cherry Jello shot” containing 75 mg of acetaminophen.

On Day 1, 3, or 7 the animals were sacrificed (Euthasol (150 mg/kg, I.P.). and in the time it took for the Euthasol to take effect, the materials were collected: bucket of ice, 15 mL tubes labeled appropriately, “RNALater” (25 mM sodium citrate at pH 5.2 and 25 mM EDTA), cutting board, scalpel blades, tweezers, surgical scissors, blue chucks, camera, and ruler tape. A picture of the wound was taken labeled with ruler tape before any surgical procedures were performed. A blue chuck was placed on the bench

and No. 15 scalpel blades used to remove the wound from the back of the animal. Then the wound was divided into: normal skin, not affected by the brand; direct burn; and the interspaces between each direct burn so, three samples were taken from each animal. See Table 1 for treatment groups. Each of these samples were harvested, minced into 1.0 mm pieces, and placed in labeled 15 mL tubes. Two sets of tissues were generated. The first set of tubes was placed in a -70 °C. "RNALater" was added to the second set of tubes and the samples were stored in a -20°C freezer to later be used for molecular study.

Tissue Extraction

Proteins were extracted in manner that would be amenable for enzymatic and immunoblotting analyses. The samples were taken out of the -70 °C freezer and approximately 100 mg of each sample was weighed out and placed into a 15 mL polypropylene round bottom tube. 2 mL of 1X Homogenization Buffer (25 mM Tris-Cl pH 7.5, 0.2 M NaCl, 3.0 mM $CaCl_2$, 0.03% Brij-35) was added and the tissue was homogenized using a Brinkmann Polytron (PT 10/35) Homogenizer with a standard saw tooth generator (20 Mm dia). The generator was rinsed with deionized water before homogenization began and in between each sample in order to prevent cross-contamination. Each tissue sample was homogenized with about 15 to 20 second pulses. The processed samples were then transferred to 1.5 ml microfuge tubes and spun at

18,000g for 20 minutes at 4°C to clarify them. The clarified extract was then transferred to a new 1.5ml tube for use in various enzymatic assays.

Protein Assay

The protein concentration was determined using the Bio-Rad Assay. This assay used an acidic solution of Coomassie Brilliant Blue G-250 dye to determine the concentration of solubilized protein in the sample. The dye binds to the protein which shifts absorbance from 465 to 595 nm. The change in color of the dye occurs in response to different amounts of protein.

Standard and sample wells were all set up in a 96-well plate. The standard wells consisted of an increasing amount of bovine serum albumin (BSA), ranging from 2 µg to 24 µg. Volumes were brought to 160 µl with water and 1X Homogenization buffer. BioRad protein assay reagent (40 µl) was added and mixed. Wells containing samples and standards contained identical amounts of the homogenization buffer to correct for artifactual contribution of the homogenization buffer to the absorbance. The plate, with the samples and standards, was then incubated and read for 5 minutes at 595 nm using the uQuant spectrophotometer (Biotek Instruments, Inc., Winooski, VT). A standard curve with a correlation of 0.9 or better was considered acceptable.

Myeloperoxidase Assay

During the acute phase of inflammation, neutrophils leave the vasculature and travel towards the site of inflammation by chemotaxis (Broughton, Janis et al., 2006). Myeloperoxidase (MPO) is a lysosomal enzyme most abundantly located in the cytoplasmic granules of neutrophils. This enzyme accounts for 5% of the total protein of neutrophils and approaches 25% of the protein within the granules themselves. Monocytes also express MPO, but these cells are much less abundant than neutrophils and express less MPO per cell than neutrophils. Therefore, this enzyme is typically regarded as a marker of neutrophils. This enzyme is synthesized as a single chain precursor developed into a tetramer consisting of two light chains and two heavy chains bound to a prosthetic heme group. MPO catalyzes the reaction of hydrogen peroxide with chloride ions to form hypochlorous acid (HClO). (Lau, Mollnau et al., 2004; Mathy-Hartert, Bourgeois et al., 1998)

The primary reaction in the MPO assay is:

$$H_2O_2 \longrightarrow H_2O + O^-$$

$$O^- + AH_2 \longrightarrow H_2O + A$$

The MPO Assay uses σ–dianisidine dyhydrochloride (AH_2) as the hydrogen donor, which combines with the oxygen radical produced from the breakdown of hydrogen peroxide. After this occurs, a colored compound is formed (A) which can be

followed spectrophotometrically to quantify the amount of myeloperoxidase in the tissue samples.

The uQuant spectrophotometer (Biotek Instruments, Inc., Winooski, VT) using KC Junior software was turned on about twenty minutes prior to use. The reagents needed were: stock MPO (Calbiochem) stored with 100 µg of MPO in 850 µL of PBS, 0.2 M Phosphate Buffer, and 50 mM Phosphate Buffer, hexadecyltrimethyl -ammonium bromide (HTAB), hydrogen peroxide, 800 µM σ – dianisidine dyhydrochloride. 85 µL aliquots of MPO were removed from the -20°C as 23.5 milliunits per µL. At pH 6.0 and 25°C one unit reduces 1 µM of hydrogen peroxide per minute. The stock MPO was diluted to 0.2 milliunit/µL. Specific amounts of MPO were added to each well of a 96 well plate. The samples were thawed and diluted to 30 µg of protein in a final volume of 150 µL of HTAB. HTAB is a detergent that was used to lyse the polymorphonuclear (PMNs) neutrophils. The protein assay was used to determine the amount of protein present in each sample. Since 5 µL of each samples were used in the protein assay, the amount of protein determined was taken and divided by 5 µL. In order to dilute the samples to 30 µg of protein in 150 µL of HTAB, 30 µg was divided by the concentration previously determined. These calculations gave the amount (µL) of sample needed to add to the wells. Then 50 µL of the samples with HTAB were added to the wells. 0.25 mg of σ – dianisidine dyhydrochloride was dissolved in 1 mL of 50 mM Phosphate Buffer and 50 µL was dispensed into the wells. The plate reader was set so that kinetic reads were taken at 5 minute intervals (12 readings) at 450 nm. Lastly, 50

µL of 0.01% hydrogen peroxide was mixed with the contents of the wells using a multi-pipettor, so as to read the plate as quickly as possible due to the fast reaction.

Concentration of Protein Samples Using Trichloroacetic Acid

It was necessary to further concentrate some extracts. This was accomplished by precipitating samples with trichloroacetic acid (TCA). The reagents needed were: 100% TCA, 20% TCA, and 100% ethanol. The amount of the sample to be placed in a 1.5 mL tube was determined from the protein assay. An equal volume of 20% TCA was added to the sample and mixed. The sample with TCA was left in the -20°C freezer for twenty minutes. The tubes were then spun at 4°C in the microcentrifuge at maximum speed for 15 minutes. The supernatant was carefully removed and discarded and the pellet retained. Washing of the pellet was accomplished by adding 100 µL of ice-cold 100% ethanol. The tube was inverted a couple of times and microfuged for 5 minutes just to ensure that the pellet was adhered to the bottom of the tube. The ethanol was then pipetted out. The pellet was air dried in Dryer in the cold room for 5 minutes. 6X Reducing Loading buffer used in the Western blot was diluted to 2X Loading Buffer. The sample was then resuspended in 36 µL of the 2X Loading Buffer. 6X Reducing Loading Buffer is composed of 3 mL [2M] of 600 mM Tris pH 6.8, 3 mL [20%] of 6.0% sodium dodecyl sulfate (SDS), 3 mL of 30% glycerol, 629 µL of 900 mM dithiothreitol (DTT), 500 µL [1%] of 0.05% *N*,*N*′-bis(2-pyridinecarboxamide)-1,2-benzene dianion (BpB), q.s. to 10 mL H_2O.

Immunoblotting (Western) Using Traditional Gel System

Polyacrylamide gels form after monomeric acrylamide is polymerized. N, N'-methylenebisacrylamide cross-links chains. Ammonium persulfate (AP) initiates this reaction and tetramethylethylenediamine (TEMED) speeds it up. In discontinuous sodium dodecyl sulfate polyacrylamide gel electrophoresis (SDS-PAGE), the samples loaded first enter the stacking gel which contains chloride ions that migrate quickly. The electrophoresis buffer contains glycine, which are less mobile. A zone is generated during electrophoresis that has low conductivity and therefore a high voltage gradient. This results in stacking of proteins between the leading and trailing ions. SDS binds most proteins in a constant weight ratio. Therefore, SDS-protein complexes migrate through the gel according to their size. A 10% gel was used in this case because this was appropriate for the observation of heme oxygenase.

The reagents needed were: 4X Stacking Gel Solution, 4X Resolving Gel Solution, 10X SDS-PAGE Running Buffer, 10% AP, 30% Bis-acrylamide stock, TEMED, 6X Loading Buffer, 10X Electroblotting Buffer, 10X Tris buffered saline Tween-20 (TBST), lowfat dried milk, primary antibody, secondary antibody, and chemiluminescence reagents (Perkin Elmer Lightning). 4X Stacking Gel solution is made up of 0.5 M Trizma Base, 0.4% SDS, and deionized water. 4X Resolving Gel solution is composed of 1.5 M Trizma Base, 0.4% SDS, and deionized water. 6X Loading Buffer consists of 600 mM Tris pH 6.8, 6.0% SDS, 30% glycerol, 900 mM DTT, 0.05% BpB, and deionized water. 10X Electroblotting Buffer is formed from 250

mM Trizma Base, 1.92 M glycine, and deionized water. Lastly, 10X TBST is created from 1.37 M NaCl, 200 mM Tris, 1% Tween, deionized water, and HCl to bring TBST to pH 7.6.

The resolving gel was made using a 1.5 mm (10 cm x 10 cm) 10% polyacrylamide gel. A traditional (dimensions including thickness 1.5mm) glass cassette and casting stand assembly were set up. The resolving gel monomer solution was prepared by combining all the reagents: 4.2 mL of deionized water, 3.3 mL of 30% acrylamide, 2.5 mL of 4X Resolving Gel Solution, and 50 µL of 10% AP, except for the TEMED. 1 mL of the resolving gel solution was transferred to a 1.5 mL tube and 25 µL of TEMED was added. Immediately 0.5 mL of the solution was poured into the assembled gel cassette acting as a plug to ensure that there were no leaks. Polymerization occurred in about 5 minutes. Then 25 µL was added to the remaining monomer solution and 6.7 mL was pipetted into the gel cassette and 1 mL of deionized water was overlaid on top of the poured resolving gel solution by dialing down of the 1000 µL pipette. The gel polymerized in about 15 minutes to 30 minutes.

While the resolving gel polymerized, the 4% stacking gel solution was prepared by combining: 3.1 mL deionized water, 0.7 mL 30% acrylamide, 1.25 mL 4X Stacking Gel Solution, and 25 µL 10% AP. Before adding the 25 µL of TEMED the solution was vacuumed for 5 minutes in order to eliminate oxygen to expedite polymerization. When polymerization of the resolving gel took place, the water on top of the gel was poured off and replaced with the stacking gel solution. After the stacking gel solution was poured, the combs were put into place. The stacking gel was allowed to polymerize for

about 30-45 minutes. Once polymerization had taken place, the combs were gently removed and placed in the assembled gel cassette into the Electrophoresis Module. The tank was filled with 1X Running Buffer. The wells were rinsed thoroughly with the 1X Running Buffer prior to loading.

Using the protein assay concentrations of the samples, 30 µg of each sample was transferred to a 1.5 mL tube and each sample brought to 30µl with deionized water. 6X Loading Buffer (6µl) was added and mixed. The samples were then heated at 95°C for 5-7 minutes in a Perkin-Elmer Thermocycler. 4-6 µL of Bio-Rad Prestained protein markers were loaded into the first lane. 30 µL of each sample was added to each remaining well. The lid was placed on the tank, making sure that the electrodes matched in color. The power supply was turned on and run at a constant voltage of 100 V. The gel ran for about 90 minutes or until blue dye reached the bottom of the gel.

The electrophoresis cassette was disassembled and in a 9 inch Pyrex dish filled with 1X Electroblot Buffer, the plates of the gel were pried apart and using a metal spatula the gel was removed from the glass plates. Sponges and filter paper were allowed to prewet in the 1X Electroblot Buffer. The Transblot cassette was placed in a second 9 inch Pyrex dish and immersed black side down in the remaining 1X Electroblot Buffer. On the black side of the cassette, a sponge, one paper filter, gel, polyvinylidene fluoride (PVDF) transfer membrane, one paper filter, and one sponge were set up. The PVDF membrane was first dipped in methanol due to the membrane being highly hydrophobic. The cassette was then placed into the transblot tank that contained an ice pack and a stirring bar. The transblot tank was set on a magnetic plate

and filled almost to the top with 1X Electroblot Buffer. The lid was put on and the electrodes were plugged into the power supply. The power supply was set to constant current at 400 mA with the unit producing about 100-125 V. The transfer went for 1 hour. The cassette was removed and the side of the membrane touching the gel was labeled with a soft lead pencil. The two pink bands of the marker were labeled and a form of ID was written on the membrane.

The membrane was blocked for 1 hour at room temperature with continual agitation with about 20 mL of 5% milk in 1X TBST. From this point on the membrane never became dry. The block was removed and rinsed quickly with 1X TBST. The primary antibody was diluted appropriately in 1X TBST and approximately 10 mL was added to the membrane. The membrane in the primary antibody was then incubated overnight at 4°C with continual rocking.

The next day the primary antibody was removed and stored at -20°C freezer and was reused several times. The membrane was washed in 1X TBST four times for 5 minutes each with 25-50 mL of 1X TBST. During the washes, the secondary antibody was diluted appropriately in 1X TBST and added to the membrane. The membrane was incubated in the secondary antibody at room temperature with continual rocking for 1 hour. The secondary antibody was removed and discarded. The membrane was again washed in 1X TBST 4 times for 5 minutes each. During the final wash, 5 mL of each of the Perkin Elmer luminal and substrate solutions were mixed (total 10 mL). After the last wash, the membrane was immersed in the luminal and substrate solution. Immediately following, the membrane was wrapped in plastic wrap and placed in a film

cassette with fluorescent crayon labels. The membrane was exposed to autorad film for 5-30 minutes and developed.

Gelatin Zymography

Gelatin zymography was used to reveal the presence of the matrix metalloprotienases (MMP), MMP-2 and MMP-9. Gelatinases are resolved by SDS-PAGE, after renaturing, the gelatinases degrade the gelatin substrate that was copolymerized into the gel. Staining with Coomasie Blue results in clear zones on the gel in the midst of a dark background. The zones of clearing represent areas in which the gelatin was degraded.

The reagents needed were: 4X Stacking Gel Solution, 4X Resolving Gel Solution, 10X SDS-PAGE Running Buffer, 10% AP, 30% Bis-acrylamide stock, 10mg/mL Gelatin, TEMED, 6X Non-Reducing Loading Buffer, 2.5% Triton X-100, 10X MMP Buffer, 0.1% Coomasie Blue, and 10% acetic acid-10% ethanol.

The resolving gel was made using a 1.5 mm (10 cm x 10 cm) 10% acrylamide gel. A traditional glass cassette and casting stand assembly were set up. The resolving gel monomer solution was prepared by combining all the reagents: 3.2 mL of deionized water, 3.3 mL of 30% acrylamide, 2.5 mL of 4X Resolving Gel Solution, 1.0 mL of 10 mg/mL Gelatin, and 50 µL of 10% AP, except for the TEMED. 1 mL of the resolving gel solution was transferred to a 1.5 mL tube and 25 µL of TEMED was added. Immediately 0.5 mL of the solution was poured into the assembled gel cassette acting as

a plug to ensure that there were no leaks. Polymerization occurred in about 5 minutes. Then 25 µL of TEMED was added to the remaining monomer solution and 6.7 mL was pipetted into the gel cassette and 1 mL of deionized water was overlaid on top of the poured resolving gel solution by dialing down of the 1000 µL pipette. The gel polymerized in about 15 to 30 minutes.

While the resolving gel polymerized, the 4% stacking gel solution was prepared by combining: 3.1 mL deionized water, 0.7 mL 30% acrylamide, 1.25 mL 4X Stacking Gel Solution, and 25 µL 10% ammonium persulfate. Before adding the 25 µL of TEMED the solution was vacuumed for 5 minutes in order to eliminate oxygen to expedite polymerization. When polymerization of the resolving gel took place, the water on top of the gel was poured off and replaced with the stacking gel solution. After the stacking gel solution was poured, the combs were put into place. The stacking gel was allowed to polymerize for about 30-45 minutes. Once polymerization had taken place, the combs were gently removed and placed in the assembled gel cassette into the Electrophoresis Module. The tank was filled with 1X Running Buffer. The wells were rinsed thoroughly with the 1X Running Buffer prior to loading.

Using the protein assay concentrations of the samples, 30 µg of each sample was transferred to a 1.5 mL tube and each sample had the appropriate amount of deionized water added, so that the same volume was added to each well. Then 1/5 volume of 6X Non- Reducing Loading Buffer was added. 4-6 µL of Bio-Rad Prestained protein markers were loaded into the first lane with 26 µL of tissue sample chosen due to high levels of protein. This addition of the same tissue sample with marker to each gel

allowed for a normalization of gel to gel variations. 30 µL of each sample was added to each remaining well. The lid was placed on the tank, making sure that the electrodes matched in color. The power supply was turned on and run at a constant voltage of 100 V. The gel ran for about 90 minutes or until blue dye reached the bottom of the gel.

The electrophoresis cassette was disassembled and in a 9 inch Pyrex dish filled with 2.5% Triton X-100, the plates of the zymogram were pried apart and using a metal spatula the zymogram was removed from the glass plates. A notch was made in the top corner of the zymogram that contained the marker. Notches were also made at the pink bands from the marker. Then the zymograms were incubated in the 2.5% Triton X-100 for 30 minutes each at room temperature on the rocker. This incubation was done twice. 10 X MMP Buffer was diluted to 1X MMP Buffer which consisted of 25 mM Tris –Cl pH 7.5, 200 mM NaCl, 3 mM $CaCl_2$, and 0.3% Brij – 35. 1X MMP Buffer was used to incubate the zymogram overnight at 37°C on the rocker.

The zymogram was removed from the 1X MMP Buffer and stained with 0.1% Coomasie Blue in 10% acetic acid and 10% ethanol for 2-4 hours on the rocker at room temperature. Destaining was done with 10% acetic acid-10% ethanol for about 1-2 hours on the rocker at room temperature. Kim-Wipes were placed in the corner of the containers in order to speed up the destaining process. When zones of clearing were very apparent, the zymogram was removed from the destaining solution and a picture was taken using a digital camera. The settings of the digital camera were consistent throughout the documenting of the zymograms: macro setting, no flash, and ISO 200 using a light box.

Assay for Collagenolytic Activity

Collagen consists of a triple helical structure. Active collagenase is an enzyme that cleaves collagen. Collagenase breaks collagen into two TC^A fragments. Above 30°C the two fragments of collagen will denature. This particular assay shows the two fragments on the gel due to utilization of radioactive collagen. Fluorography is used for detecting the radioactive labeled collagen activity in the assay. Radiation is emitted from substances in this case collagen that are radioactively labeled. This radiation excites a molecule, also known as a fluor, in the gel. The excited fluor then relaxes back down to the ground state and emits a photon of visible light that is detected by a film. Then the film is developed and the bands are portrayed. This technique allows for increased sensitivity to weak radiation signals. (Waterborg et al., 1994; Laskey, 2003)

The reagents needed were: dialyzed ^{14}C labeled collagen (Type I), 10X MMP Buffer, 500 mM EDTA, 50 mM aminophenylmercuric acetate (APMA) made fresh in 0.1 N NaOH, 6% SDS-PAGE gel, 6X Reducing Loading Buffer, 10% acetic acid-10% ethanol, and Amplify.

Master mixes were set up on ice using 0.5 mL microfuge tubes. There were three tubes per sample: negative, active, and total. The negative contained 30 µL of 1X MMP Buffer, 20 µL of sample, 2 µL of ethylenediamene tetraacedic acid (EDTA), and 50 µL of ^{14}C-collagen. The active contained 30 µL of 1X MMP Buffer, 20 µL of sample, and 50 µL of ^{14}C-collagen. The total contained 30 µL of 1X MMP Buffer, 20 µL of sample, 3 µL of aminophenylmercuric acetate (APMA), and 50 µL of ^{14}C

-collagen. Once these samples were prepared, they were placed in the Thermocycler at 30°C for 1 hour, 4 hours, and overnight. After 1 hour a 30 µL aliquot was taken out and added to a new tube containing 6 µL of 6X Reducing Loading Buffer to stop the reaction. This same aliquot was done after 4 hours and then overnight. The tubes taken out after 1 hour and 4 hours were then stored at -20°C until the last aliquot was collected. When all the aliquots were ready to be run, a 6% SDS-PAGE gel was made.

The resolving gel was made using a 1.5 mm (10 cm x 10 cm) 6% acrylamide gel. A traditional glass cassette and casting stand assembly were set up. The resolving gel monomer solution was prepared by combining all the reagents: 5.5 mL of deionized water, 2.0 mL of 30% acrylamide, 2.5 mL of 4X Resolving Gel Solution, and 50 µL of 10% AP, except for the TEMED. 1 mL of the resolving gel solution was transferred to a 1.5 mL tube and 25 µL of TEMED was added. Immediately 0.5 mL of the solution was poured into the assembled gel cassette acting as a plug to ensure that there were no leaks. Polymerization occurred in about 5 minutes. Then 25 µL was added to the remaining monomer solution and 6.7 mL was pipetted into the gel cassette and 1 mL of deionized water was overlaid on top of the poured resolving gel solution by dialing down of the 1000 µL pipette. The gel polymerized in about 15 to 30 minutes.

While the resolving gel polymerized, the 4% stacking gel solution was prepared by combining: 3.1 mL deionized water, 0.7 mL 30% acrylamide, 1.25 mL 4X Stacking Gel Solution, and 25 µL 10% ammonium persulfate. Before adding the 25 µL of TEMED the solution was vacuumed for 5 minutes in order to eliminate oxygen to expedite polymerization. When polymerization of the resolving gel took place, the

water on top of the gel was poured off and replaced with the stacking gel solution. After the stacking gel solution was poured, the combs were put into place. The stacking gel was allowed to polymerize for about 30-45 minutes. Once polymerization had taken place, the combs were gently removed and placed in the assembled gel cassette into the Electrophoresis Module. The tank was filled with 1X Running Buffer. The wells were rinsed thoroughly with the 1X Running Buffer prior to loading.

The samples were heated at 95°C for 5 minutes and run on the gel with 30 µL of sample per well using 4-6 µL of marker in Lane 1 only. The gel was electrophoresed at 100 V for about 45 minutes. The gels were removed from the glass and fixed in 10% acetic acid-10% ethanol for 10-15 minutes at rocker on room temperature or until the dark blue band at the bottom of the gel turned a yellow color. The gels were then incubated in about 25 mL of Amplify for 20 minutes on the rocker at room temperature. About 45 minutes prior to gel drying, the gel dryer was turned on. The gels were placed on two sheets of filter paper, covered with saran wrap, and placed on the dryer for 1 hour. Immediately following, the gel was wrapped in plastic wrap and placed in a film cassette with fluorescent crayon labels. The gel was exposed to film for about 2 days in the -70°C freezer and developed.

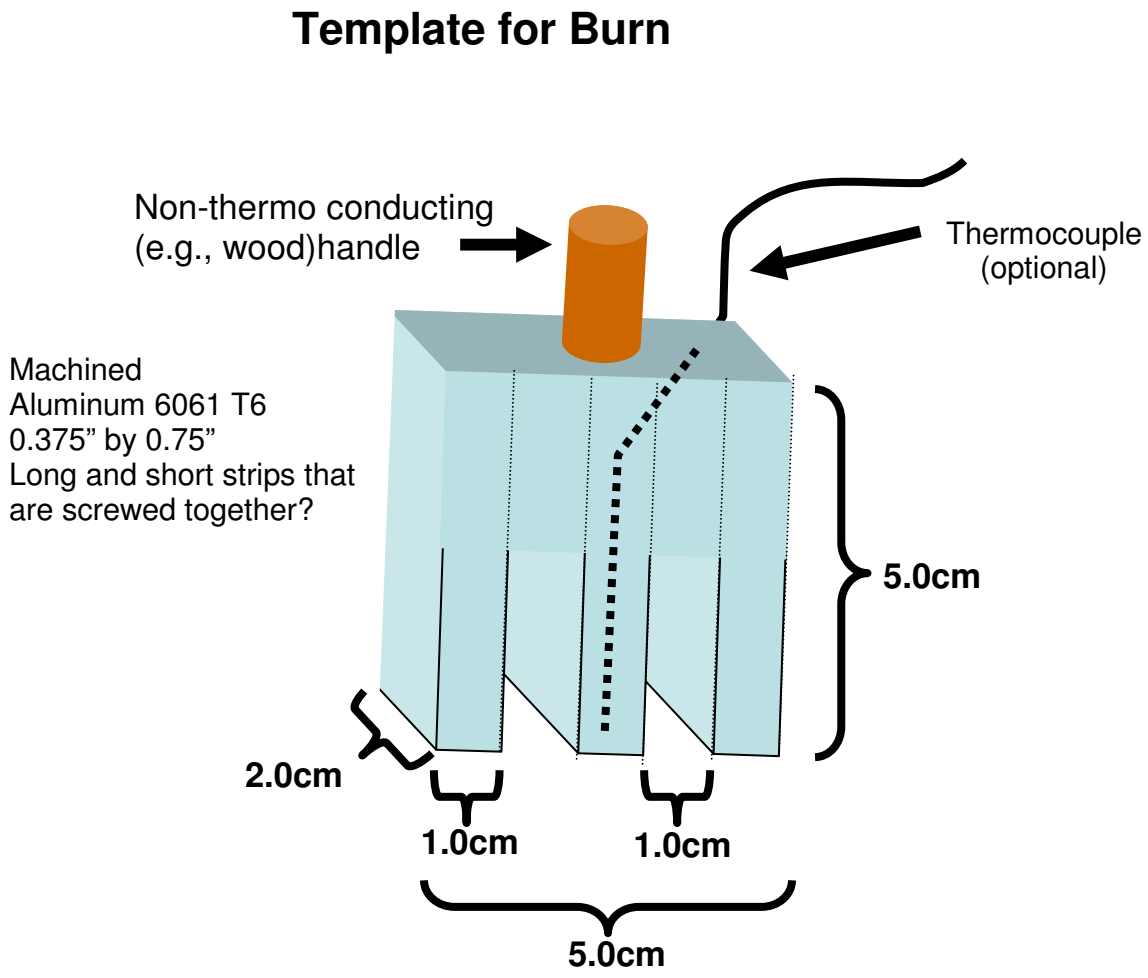

Figure 4: Template for Burn Wound

Table 1: Treatment Groups for Burn Wounding

Treatment Groups				
Groups	**Treatment**	**Day 1**	**Day 3**	**Day 7**
1	Burned, untreated	N=8	n=7	n=7
2	Burned, 5mg/kg CoPP	N=8	n=7	n=7
3	Burned, 30μM/kg SnPP	N=7	n=7	n=9

Results

Surgery and Animal Survival

Full-thickness thermal injury was generated using an established procedure with some modification (Ehrlich et al., 1992). In the original model, a brass probe consisting of a 55 x 19 mm rectangle with three 5 mm wide transverse notches was used to generate a row of four 10 x 19 mm full-thickness burns. Because of the size of this probe, it was found to be difficult to achieve a relative uniform burn. Therefore, the probe used in this study was modified to consist of a 40 mm x 20mm rectangle containing two 5 mm-wide transverse notches.

A pilot was performed on a small group of animals to establish optimal contact time required for obtaining a reproducible full-thickness thermal injury with minimal involvement of the underlying muscle. Animals were anesthetized with inhalant isoflurane and provided buprenorphine analgesia subcutaneously (sc). A rectangular brass probe was equilibrated to 100°C. The heated probe was applied to the depilated back of the anesthetized animals. Probes were allowed to "balance" on the skin for 30, 35, 40, and 45 seconds before removing. The wounds were examined on days post wounding 1 and 3. It was determined that application of the probe for 45 seconds achieved the desired burn severity. This procedure was used on all 54 animals in this study. Mortality was less than 2% (1/54). The total surface area of the burn injury was less than 4% of total body surface area.

On some occasions, while using the Nair product to eliminate the rats' hair prior to injury, all the hair was not completely removed. This could have had a slight effect on the small differences between burn wounds.

The rats were examined twice daily and to provide analgesia. All of the animals appeared normal, alert, and experiencing little pain given that pain medications were administered daily. Documentation of the injury on the animals was made daily. The majority of the animals did not seem to aggravate their wounds and only very few appeared to be worse after healing should have already set in. A picture was taken immediately after each animal was injured. Wounds were also photo-documented on sacrifice Day 1, Day 3, and Day 7 following injury. See Figure 6. Following euthansia, normal skin, skin subjected to direct application of the probe (direct) and skin representing the interspace was harvested. Tissues were bisected with portions snap frozen and stored at -70°C or placed in "RNALater" and stored at -20°C.

Measurement of Burn Conversion

Areas of necrosis within the interspace regions of wounds taken at harvest were determined by planimetry using SigmaScan. Each photograph was calibrated using a size reference placed on each wound. Areas of frank necrosis were then determined. As can be seen in figure 7, in general, wounds in animals treated with Co PP contained smaller areas of frank necrosis than either the Sn PP or untreated groups. For the Co PP

treated group, there was a statistically significant difference ($p<0.05$, ANOVA, Tukeys) on days 3 and 7 compared to either of the other two groups.

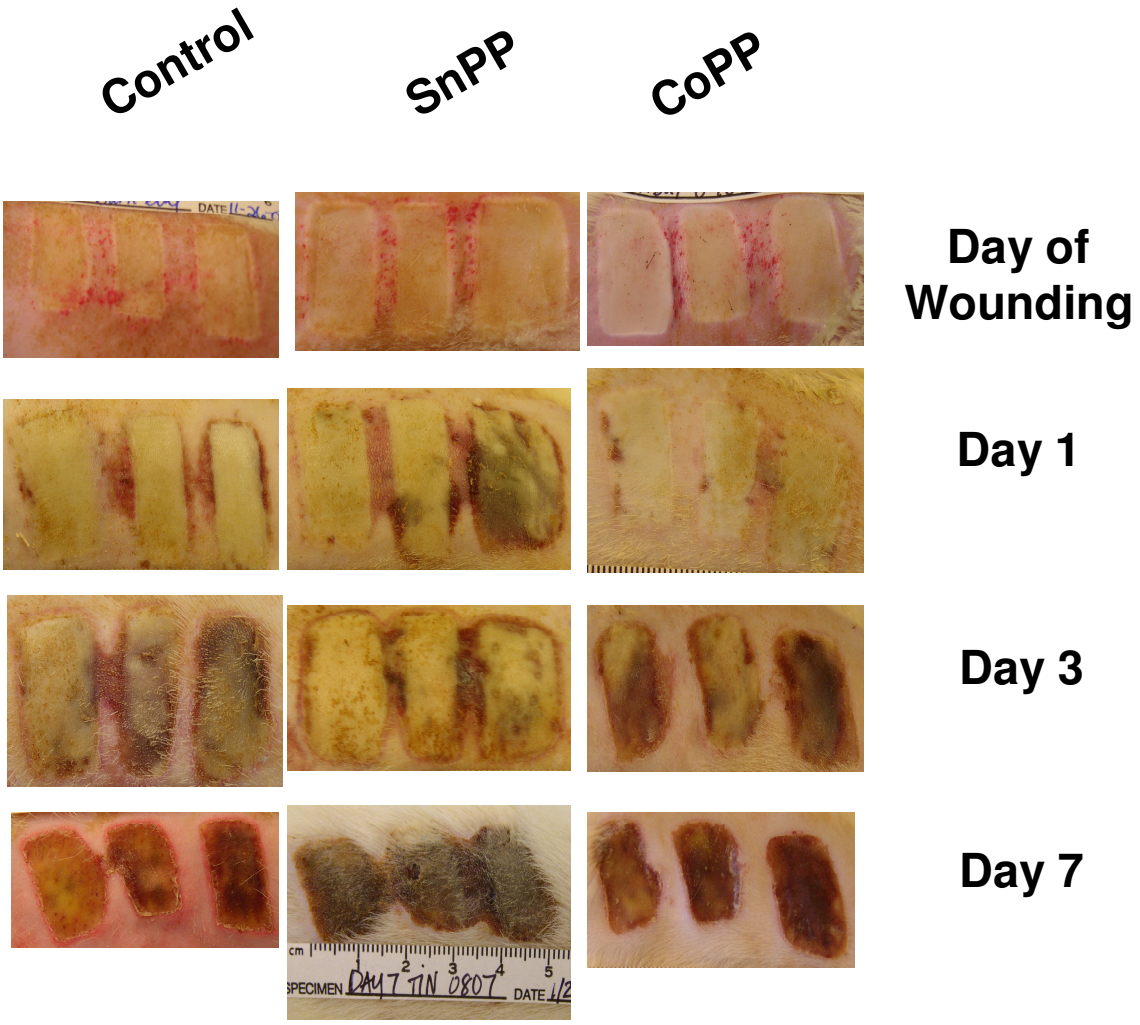

Figure 6: Representative Burns on Days 0, 1, 3, and 7 Post Wounding

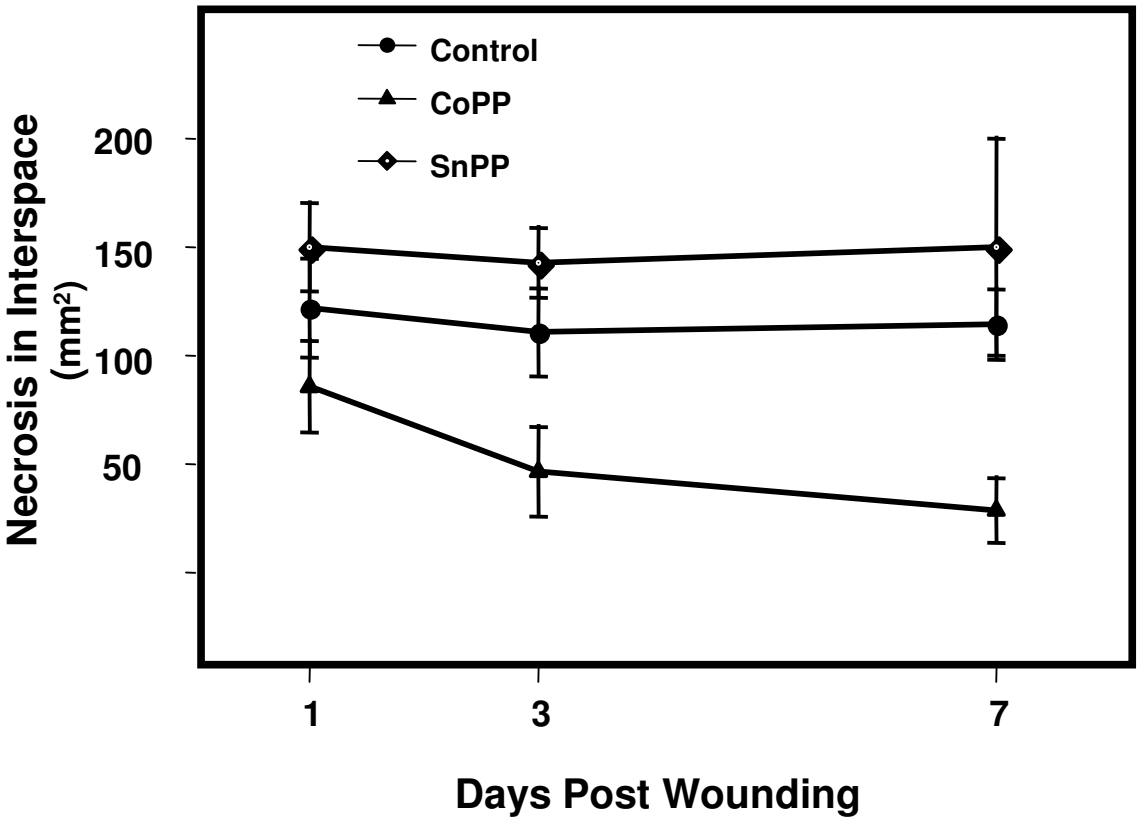

Figure 7: Mean Levels of Necrosis

BCA Assay for Protein Concentration

Tissues were thawed on ice and then extracted as described in the Methods. Concentrations of protein extracts were determined using the bicinchoninic acid protein assay using bovine serum albumin to generate a standard curve. This assay has been adapted to a 96-well format to minimize consumption of materials. The protein standard curve shown in figure 8 on page 42 was very accurate from 2 – 24 µg. There was one point (under 2 µg) on the standard curve that appeared to not be consistent with the rest of the points, but when taking that specific point out; the R-squared value became 0.9894. $R^2 = 1$ is considered to be a perfect standard curve. This assay showed that there was an abundant amount of protein in the samples. By ensuring that protein was in each sample, the multitudes of subsequent tests were able to be performed.

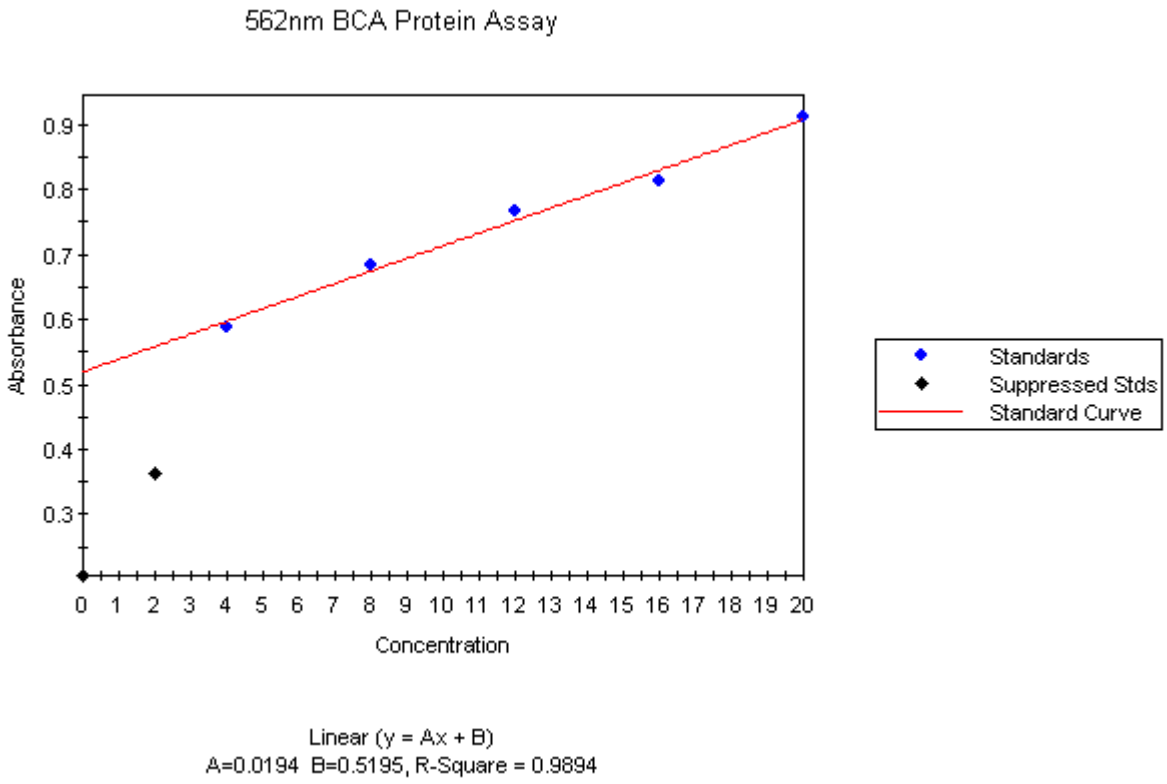

Figure 8: Protein Assay Standard Curve Generated from Tissue Samples; the curve was linear between 2 and 24 µg of protein

Western Blot for Heme Oxygenase - 1 Levels

The heme oxygenase – 1 protein levels were determined using immunoblotting. HO-1 migrated as a 32 kDa protein. A composite of HO-1 expression on Day 1 is shown in figure 9. In animals not treated with heavy metal protoporphyrins there is no detectable expression of HO-1 in non-burned skin. In contrast there is significant expression of HO-1 in the interspace region. This was expected as HO-1 is a stress response protein. Typically, there were lower levels of HO-1 present in tissues representing full-thickness burns. As these tissues are nonviable, this was an expected outcome. HO-1 expression in tissues from animals treated with either heavy metal protoporphyrin revealed a significantly different pattern. As expected, heavy metal protoporphyrins induced global expression of HO-1. Somewhat unexpectedly, HO-1 levels were consistently higher in tissues from animals treated with Co PP than with Sn PP (Figures 10-12). *In vitro* studies in this laboratory have demonstrated that carbon monoxide, one of the products generated by HO-1, can act in a positive feedback manner on HO-1 expression (Kulina, R., 2008). Thus, the higher levels observed in animals treated with Co PP may be explained by this. A less likely explanation is that Co PP's ability to inhibit necrosis may in turn permit greater expression of HO-1. However, the differential response to the heavy metal protoporphyrins is observed in non-burned tissues (Figure 11). Statistical analysis was achieved using the program, SigmaStat. ANOVA (Tukeys) tests were performed for direct burn tissue, non-burned tissue, and interspace tissue. See Tables 2-4.

Beginning with tissue samples from the directly burned skin on Day 1 and Day 3 showed similar results. Cobalt PP HO – 1 levels were the highest, while in the control groups, the lowest levels were observed. Tin PP showed HO – 1 levels mid – range and the untreated animals had the lowest levels of HO – 1. The amount of HO – 1 was greater in every group on Day 3 compared to Day 1. The final surgery day, Day 7, showed the cobalt PP group with the highest levels of HO – 1, which appears to be very consistent. The untreated group has fairly high levels of HO – 1. Lastly, the tin PP treated animals had the lowest amount of HO – 1.

Skin tissue samples (uninjured tissue) on Day 1, the animals treated with cobalt PP had the highest level of HO – 1. Untreated animals had the lowest concentration of HO – 1 and the animals treated with tin PP also had very low levels. Day 3 skin HO – 1 level was again highest in cobalt PP and lowest in non – treated animals. The HO – 1 level for Tin PP were slightly higher than those for Day 1, but again low. Lastly, the HO – 1 levels for skin Day 7 again had cobalt PP treated animals with the highest concentration, but tin PP with the lowest concentration. The non – treated animals had an increase compared to Day 1 and Day 3.

The interspace tissue samples for Day 1 and Day 3 show the highest level of heme oxygenase – 1 in the tissue treated with cobalt PP. The lowest level of HO – 1 is apparent in the control group and tin PP HO – 1 levels ranged in the middle of the control and cobalt PP treated animals. Although, Day 3 tin PP HO – 1 levels were slightly higher than those of Day 1. The interspace samples for Day 7 were slightly different. The tissue treated with cobalt PP again had the highest level of HO – 1. Tin

PP had the lowest level of HO – 1 and the untreated animals showed the middle range of HO – 1 levels.

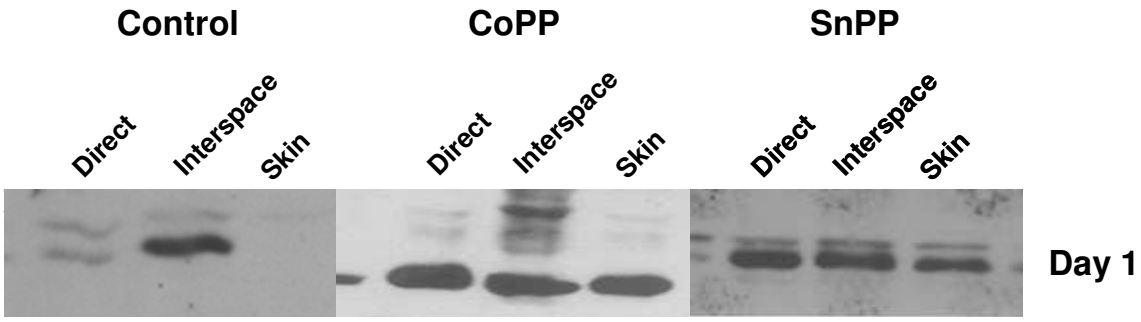

Figure 9: Representative Immunoblot - HO-1 Protein Expression on Day 1

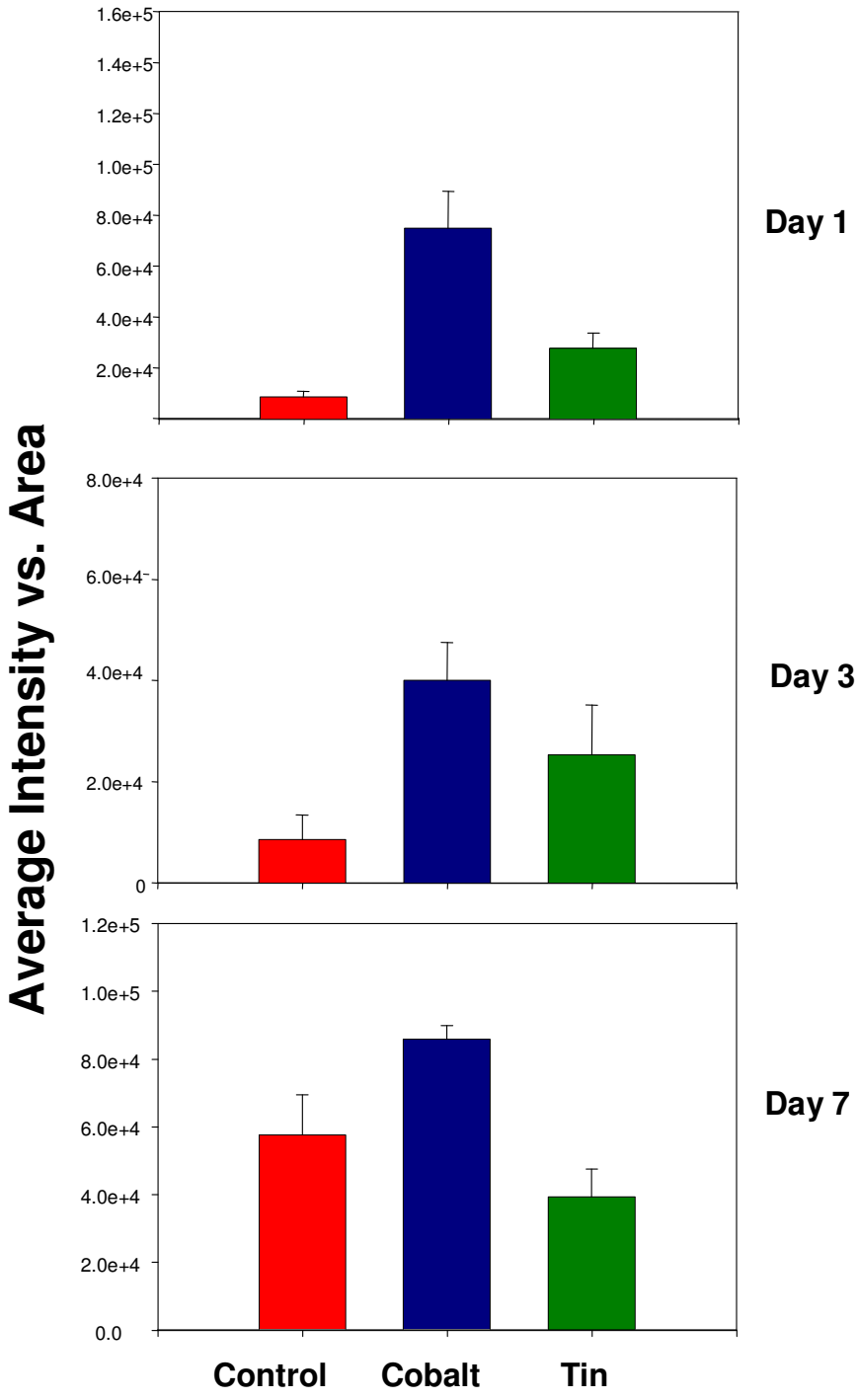

Figure 10: HO-1 Protein Levels in Full-thickness Burns

Table 2: Statistical Analysis (ANOVA) for HO-1 Levels in Direct Burn Tissues

One Way Analysis of Variance Thursday, December 11, 2008, 19:26:45

Data source: Data 1 in Notebook

Normality Test: Passed (P = 0.061)

Equal Variance Test: Failed (P = 0.035)

Test execution ended by user request, ANOVA on Ranks begun

Kruskal-Wallis One Way Analysis of Variance on Ranks Thursday, December 11, 2008, 19:26:45

Data source: Data 1 in Notebook

Group	**N**	**Missing**
Control Day 1	8	0
Cobalt Day 1	8	0
Tin Day 1	7	0
Control Day 3	7	0
Cobalt Day 3	7	0
Tin Day 3	7	0
Control Day 7	7	0
Cobalt Day 7	7	0
Tin Day 7	6	0

Group	**Median**	**25%**	**75%**
Control Day 1	8397.000	3072.000	14675.500
Cobalt Day 1	68063.500	42127.500	108685.000
Tin Day 1	27057.000	16770.250	39450.500
Control Day 3	4042.000	1992.750	8368.750
Cobalt Day 3	43827.000	20439.250	50667.250
Tin Day 3	13265.000	9340.500	39747.750
Control Day 7	68678.000	30986.000	78767.000
Cobalt Day 7	84808.000	81665.000	91055.500
Tin Day 7	40430.000	32044.000	54506.000

H = 39.032 with 8 degrees of freedom. (P = <0.001)

The differences in the median values among the treatment groups are greater than would be expected by chance; there is a statistically significant difference (P = <0.001)

To isolate the group or groups that differ from the others use a multiple comparison procedure.

All Pairwise Multiple Comparison Procedures (Dunn's Method):

Comparison	**Diff of Ranks**	**p**	**Q**	**P<0.05**
Cobalt Day 7 vs Control Day 3	45.429	9	4.565	Yes
Cobalt Day 7 vs Control Day 1	43.196	8	4.483	Yes
Cobalt Day 7 vs Tin Day 3	31.429	7	3.158	No
Cobalt Day 7 vs Tin Day 1	29.429	6	2.957	No Test Needed
Cobalt Day 7 vs Tin Day 7	23.238	5	2.243	No Test Needed
Cobalt Day 7 vs Cobalt Day 3	21.000	4	2.110	No Test Needed
Cobalt Day 7 vs Control Day 7	14.143	3	1.421	No Test Needed
Cobalt Day 7 vs Cobalt Day 1	8.196	2	0.851	No Test Needed
Cobalt Day 1 vs Control Day 3	37.232	8	3.864	Yes
Cobalt Day 1 vs Control Day 1	35.000	7	3.760	Yes

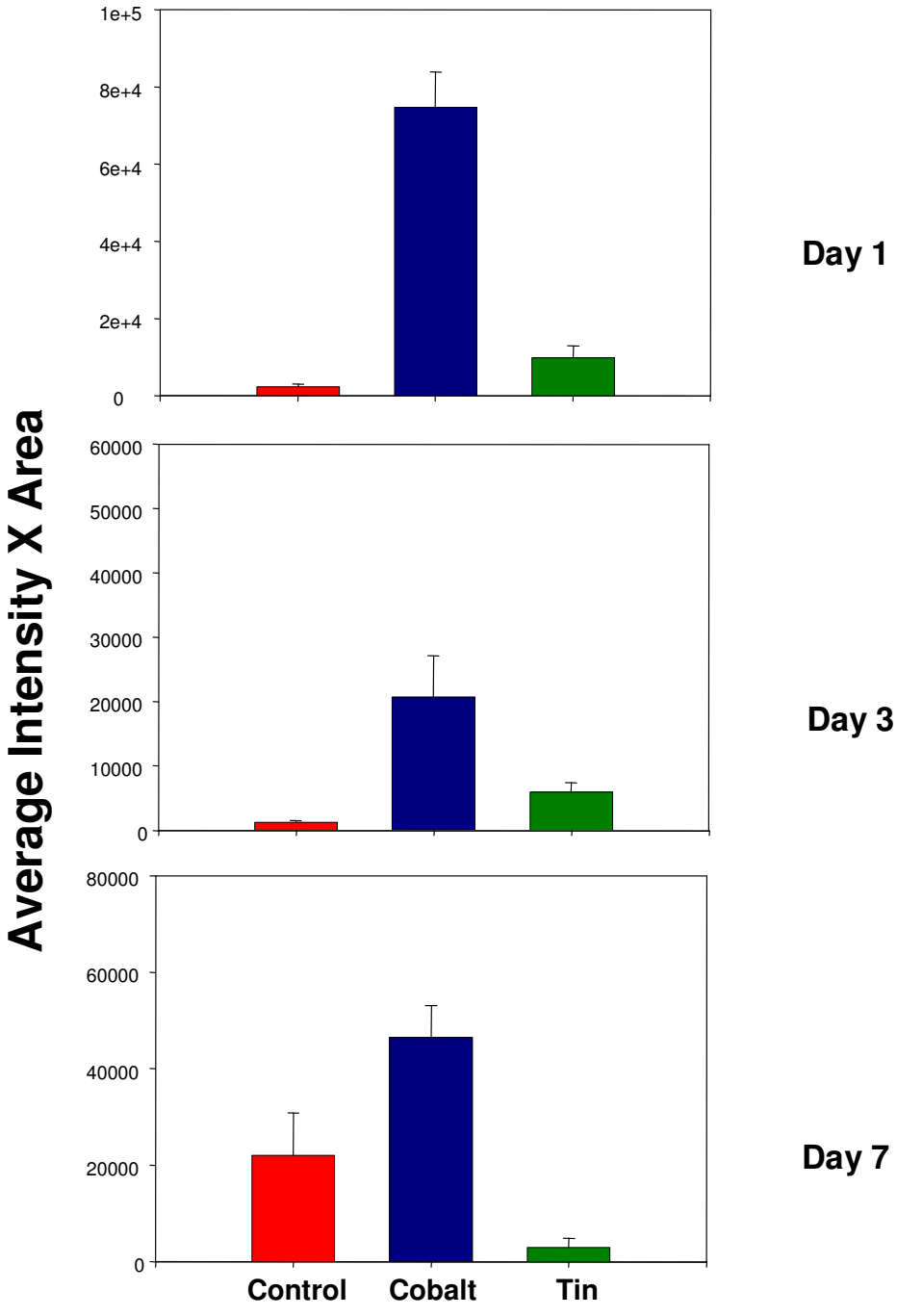

Figure 11: HO-1 Protein Levels in Unburned Skin

Table 3: Statistical Analysis (ANOVA) for HO-1 Levels in Unburned Tissues

One Way Analysis of Variance Thursday, December 11, 2008, 19:46:21

Data source: Data 1 in Notebook

Normality Test: Failed (P = <0.001)

Test execution ended by user request, ANOVA on Ranks begun

Kruskal-Wallis One Way Analysis of Variance on Ranks Thursday, December 11, 2008, 19:46:21

Data source: Data 1 in Notebook

Group	**N**	**Missing**
Control Day 1	8	0
Cobalt Day 1	8	0
Tin Day 1	7	0
Control Day 3	7	0
Cobalt Day 3	7	0
Tin Day 3	7	0
Control Day 7	7	0
Cobalt Day 7	7	0
Tin Day 7	6	0

Group	**Median**	**25%**	**75%**
Control Day 1	1673.000	1148.000	3236.500
Cobalt Day 1	84846.500	73776.000	87035.000
Tin Day 1	6999.000	3667.500	12697.750
Control Day 3	830.000	459.500	2020.750
Cobalt Day 3	23963.000	5013.250	31789.000
Tin Day 3	5255.000	2406.250	9653.500
Control Day 7	15304.000	6636.250	25079.250
Cobalt Day 7	47388.000	36323.000	62480.500
Tin Day 7	1672.500	0.000	3437.000

H = 45.610 with 8 degrees of freedom. (P = <0.001)

The differences in the median values among the treatment groups are greater than would be expected by chance; there is a statistically significant difference (P = <0.001)

To isolate the group or groups that differ from the others use a multiple comparison procedure.

All Pairwise Multiple Comparison Procedures (Dunn's Method):

Comparison	**Diff of Ranks**	**p**	**Q**	**P<0.05**
Cobalt Day 1 vs Control Day 3	47.393	9	4.918	Yes
Cobalt Day 1 vs Control Day 1	42.500	8	4.565	Yes
Cobalt Day 1 vs Tin Day 7	42.250	7	4.202	Yes
Cobalt Day 1 vs Tin Day 3	31.821	6	3.302	Yes
Cobalt Day 1 vs Tin Day 1	25.393	5	2.635	No
Cobalt Day 1 vs Cobalt Day 3	21.107	4	2.190	No Test Needed
Cobalt Day 1 vs Control Day 7	18.250	3	1.894	No Test Needed
Cobalt Day 1 vs Cobalt Day 7	6.679	2	0.693	No Test Needed
Cobalt Day 7 vs Control Day 3	40.714	8	4.091	Yes
Cobalt Day 7 vs Control Day 1	35.821	7	3.717	Yes
Cobalt Day 7 vs Tin Day 7	35.571	6	3.434	Yes
Cobalt Day 7 vs Tin Day 3	25.143	5	2.526	No

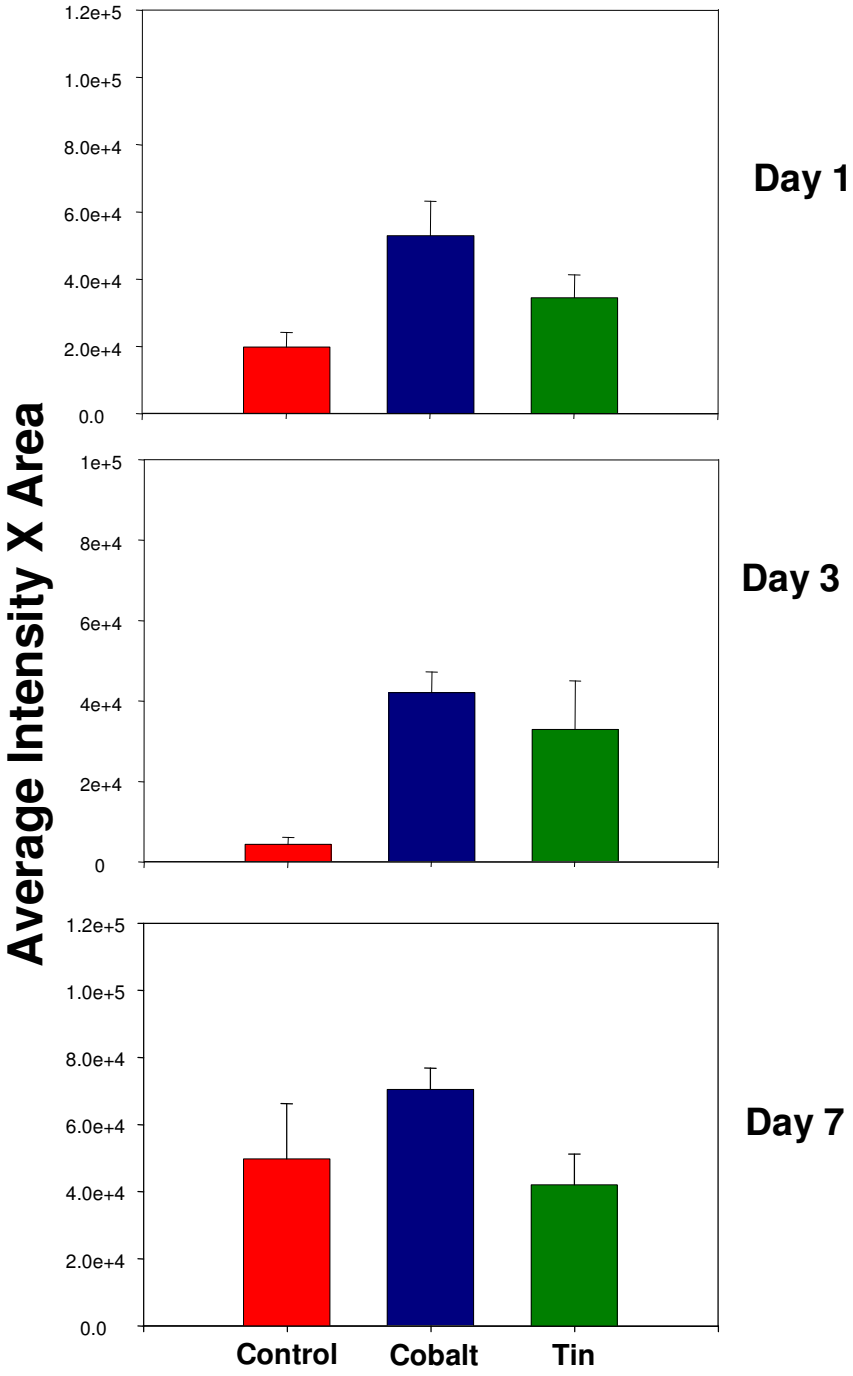

Figure 12: HO-1 Protein Levels in Interspace Tissues

Table 4: Statistical Analysis (ANOVA) for HO-1 Levels in Interspace Tissue

One Way Analysis of Variance Thursday, December 11, 2008, 20:10:49

Data source: Data 1 in Notebook

Normality Test: Passed (P = 0.168)

Equal Variance Test: Passed (P = 0.062)

Group	**N**	**Missing**
Control Day 1	8	0
Cobalt Day 1	8	0
Tin Day 1	7	0
Control Day 3	7	0
Cobalt Day 3	7	0
Tin Day 3	7	0
Control Day 7	7	0
Cobalt Day 7	7	0
Tin Day 7	6	0

Group	**Mean**	**Std Dev**	**SEM**
Control Day 1	19666.000	12095.603	4276.441
Cobalt Day 1	52713.750	29197.309	10322.808
Tin Day 1	34347.143	18103.927	6842.641
Control Day 3	4236.571	4643.180	1754.957
Cobalt Day 3	41902.857	13852.335	5235.691
Tin Day 3	32908.571	31924.946	12066.496
Control Day 7	49755.286	43532.157	16453.609
Cobalt Day 7	70471.143	16860.181	6372.549
Tin Day 7	42003.167	22585.685	9220.567

Power of performed test with alpha = 0.050: 0.971

Source of Variation	**DF**	**SS**	**MS**	**F**	**P**
Between Treatments	8	21207898335.238	2650987291.905	4.559	<0.001
Residual	55	31980361643.762	581461120.796		
Total	63	53188259979.000			

The differences in the mean values among the treatment groups are greater than would be expected by chance; there is a statistically significant difference (P = <0.001).

All Pairwise Multiple Comparison Procedures (Tukey Test):

Comparisons for factor:

Comparison	**Diff of Means**	**p**	**q**	**P<0.05**
Cobalt Day 7 vs. Control Day 3	66234.571	9	7.267	Yes
Cobalt Day 7 vs. Control Day 1	50805.143	9	5.757	Yes
Cobalt Day 7 vs. Tin Day 3	37562.571	9	4.121	No
Cobalt Day 7 vs. Tin Day 1	36124.000	9	3.964	No
Cobalt Day 7 vs. Cobalt Day 3	28568.286	9	3.135	No
Cobalt Day 7 vs. Tin Day 7	28467.976	9	3.001	No
Cobalt Day 7 vs. Control Day 7	20715.857	9	2.273	No
Cobalt Day 7 vs. Cobalt Day 1	17757.393	9	2.012	No
Cobalt Day 1 vs. Control Day 3	48477.179	9	5.493	Yes
Cobalt Day 1 vs. Control Day 1	33047.750	9	3.876	No
Cobalt Day 1 vs. Tin Day 3	19805.179	9	2.244	No
Cobalt Day 1 vs. Tin Day 1	18366.607	9	2.081	No
Cobalt Day 1 vs. Cobalt Day 3	10810.893	9	1.225	No

Inflammation (Myeloperoxidase and MMP Levels)

The myeloperoxidase (MPO) assay was used to provide an indication of the amount of neutrophils located in tissue. In response to injury, neutrophils are recruited to the site of trauma. Neutrophils contain granules which hold myeloperoxidase. MPO accounts for 5% of the total protein content of neutrophils. This enzyme is also found in lesser amounts in monocytes. MPO specifically converts hydrogen peroxide to hypohalous acids in order to prevent neutrophils from apoptosis. This assay was used to determine neutrophil levels and thus provide an indication of inflammation in each group of tissue: skin, interspace, and direct. A representative standard curve using purified neutrophil MPO is shown in figure 13.

MPO activity in the skin samples at all three time points was very low and consistent with almost all the samples. The data ranged from -12.4 milliunits/mg to 1.2 milliunits/mg with one exception at 8.8 milliunits/mg. From 0 to 80 milliunits of MPO the assay was linear with a R – squared value of 0.9841.

In contrast to the skin, MPO activity in the interspace samples was high (figure 14). Statistical analysis was achieved using ANOVA (Tukey) test. See Table 5. MPO levels ranged from 9.6 milliunits/mg to 583.0 milliunits/mg. The R – squared value was 0.9957. Due to some of these extremely high data, certain samples significantly over 200 milliunits/mg were recalculated. By diluting specific tissue samples, another assay was performed in order to show more accurate results. The data ranged from 1.2

milliunits/mg to 253.3 milliunits/mg with only two outliers in the negative. The R – squared value for the recalculated data was 0.9904.

Lastly, the activity in the direct samples was high. The R – squared value for the graphed data was 0.9949. The data ranged from 9.6 milliunits/mg to 464.0 milliunits/mg. The last four points were taken out of the data just as in the skin samples because when adding 0.1% hydrogen peroxide due to human error, the reaction occurred too quickly before being placed in the spectrometer and therefore skewed the data. Just as in the interspace samples, specific samples were recalculated due to extremely high levels of MPO and were diluted to increase the accuracy of results. The recalculated data ranged from -2.9 milliunits/mg to 66.1 milliunits/mg. The R – squared value for the recalculated data was 0.9879.

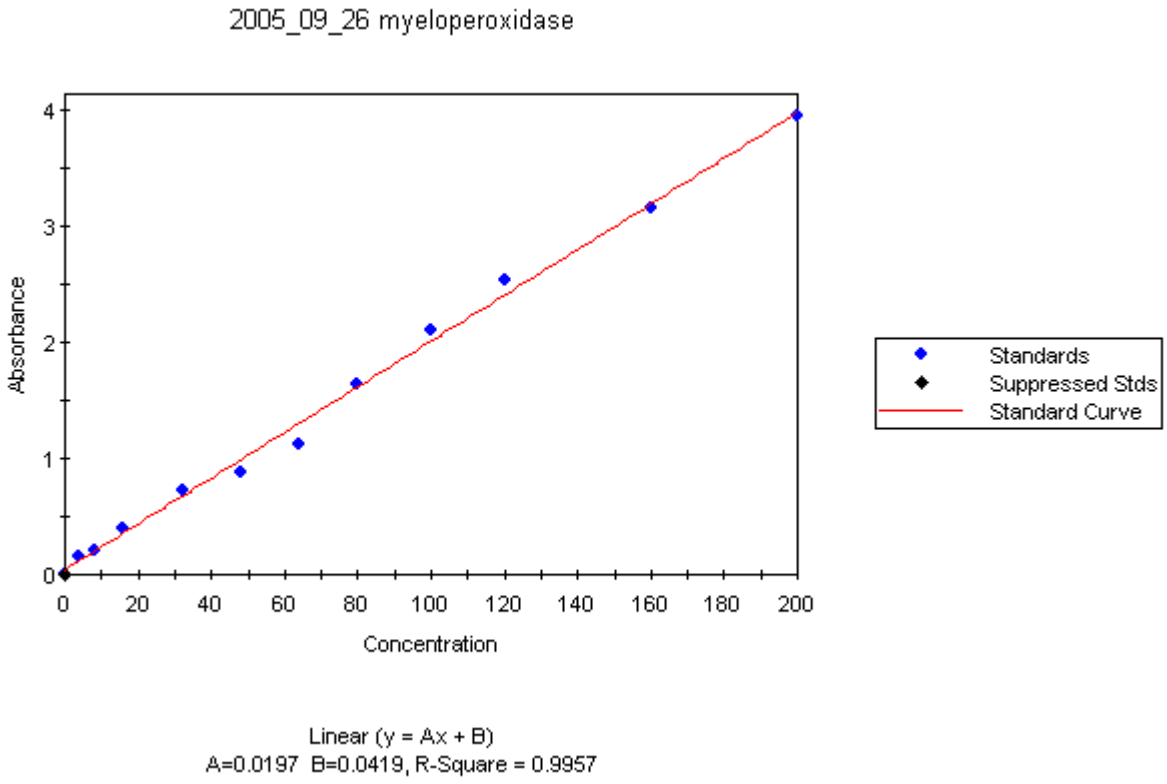

Figure 13: Representative Myeloperoxidase Standard Curve

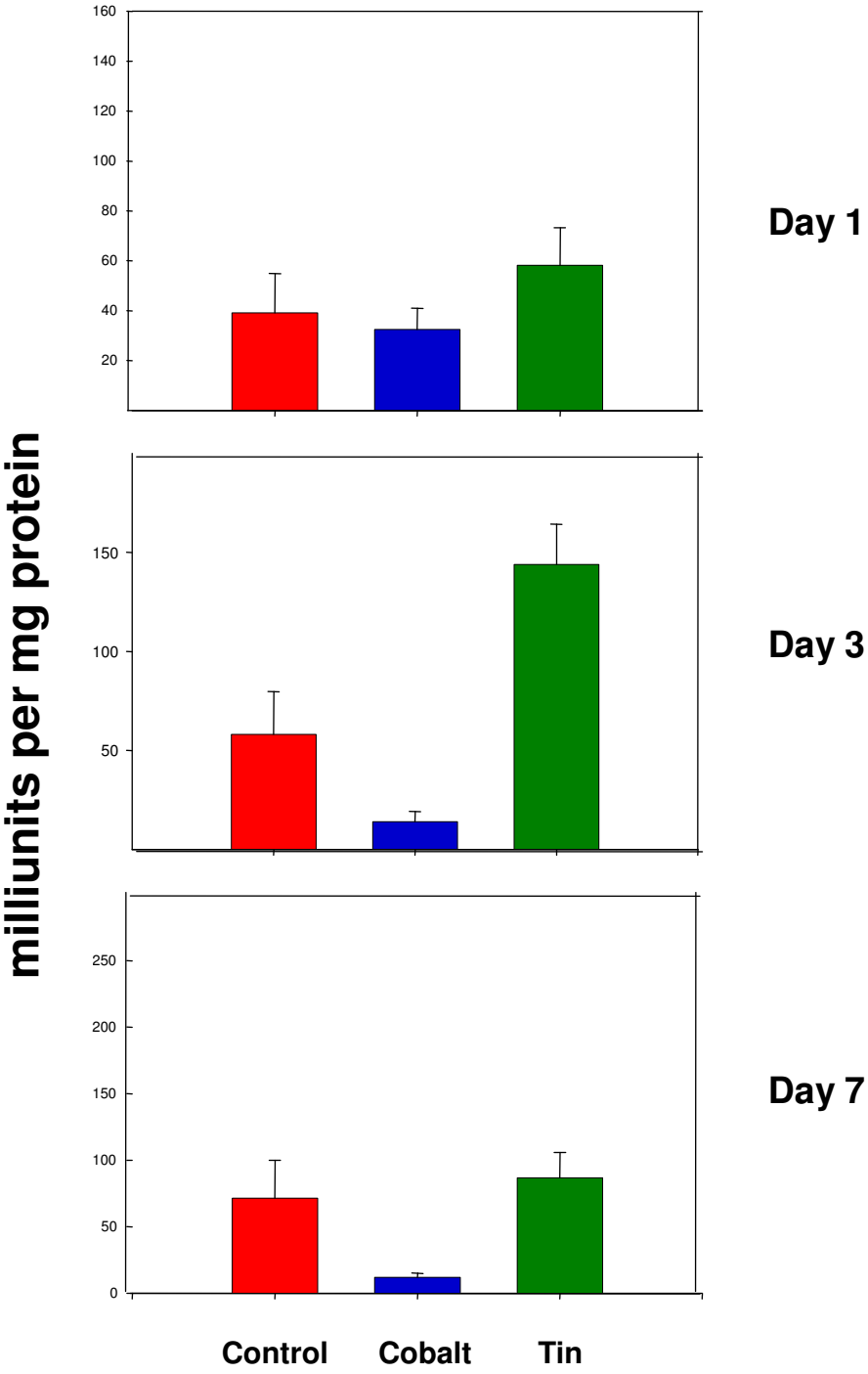

Figure 14: Mean Myeloperoxidase Activities in Interspace Tissues

Table 5: Statistical Analysis (ANOVA) for MPO Assay Interspace Tissues

One Way Analysis of Variance Friday, December 12, 2008, 11:09:42

Data source: Data 1 in Notebook

Normality Test: Failed (P = 0.012)

Test execution ended by user request, ANOVA on Ranks begun

Kruskal-Wallis One Way Analysis of Variance on Ranks Friday, December 12, 2008, 11:09:42

Data source: Data 1 in Notebook

Group	**N**	**Missing**
Control Day 1	8	0
Tin Day1	7	0
Cobalt Day 1	8	0
Control Day 3	7	0
Tin Day 3	7	0
Cobalt Day 3	7	0
Control Day 7	7	0
Tin Day 7	6	0
Cobalt Day 7	7	0

Group	**Median**	**25%**	**75%**
Control Day 1	2.570	1.590	3.595
Tin Day1	1.970	1.333	2.820
Cobalt Day 1	2.835	1.310	4.750
Control Day 3	2.010	0.665	2.945
Tin Day 3	3.020	2.700	3.460
Cobalt Day 3	1.830	1.293	2.885
Control Day 7	2.070	1.875	2.543
Tin Day 7	3.060	2.130	3.440
Cobalt Day 7	1.070	0.498	1.948

H = 14.802 with 8 degrees of freedom. (P = 0.063)

The differences in the median values among the treatment groups are not great enough to exclude the possibility that the difference is due to random sampling variability; there is not a statistically significant difference (P = 0.063)

Gelatin zymography is used to study certain enzymes in tissues and cells that degrade extracellular matrix. The enzymes of particular interest in this study are MMP's, specifically MMP – 9. MMP's degrade the gelatin that was added into the gel. Using the Coomasie Blue dye, the clear zones in the gel are exposed showing enzymes capable of degrading the gelatin. When analyzing the zymograms, there are two bands that appear on the gels that represent the presence of MMP – 9. The top band portrays the latency or pro form of MMP - 9, while the bottom band portrays the active form. By observing the data, it was determined that by averaging the intensities of both bands using densitometric scoring in SigmaScan gave the most accurate results. Each intensity was normalized using the background on each gel corresponding with the samples. A standard graph was generated using a sample that had such a large amount of enzyme. The specific sample used with the normal 30 µg sample blew out the lane on the gel, which means degraded almost the whole lane. Smaller and smaller increments of this specific tissue sample were used to create the standard. See Figure 15.

The two standards showed a very consistent set of data. This gave a high confidence that the zymograms carried out were giving accurate results. Only a select few skin and direct tissue samples were analyzed, whereas all interspace samples were evaluated.

In the skin tissue samples, Day 1, 3, and 7 all showed the highest level of MMP – 9 in the control (untreated) samples. Day 1 showed Co PP and Sn PP treated had the same levels of MMP – 9. Day 3 had Co PP treated tissue trailing slightly behind the untreated group. The Sn PP treated group on Day 3 was also high, but had the lowest

levels of MMP – 9 compared to the other groups. Day 7 showed the Co PP treated tissue with the lowest levels and Sn PP levels high, but not has high as the untreated group. In the untreated skin tissue, MMP – 9 levels were fairly high and around the same for each day. There was not much fluctuation. The Co PP treated tissue had the highest levels of MMP – 9 on Day 3 and the lowest levels on Day 7. Sn PP treated samples had the highest levels of MMP – 9 on Day 7 and the lowest levels on Day 1.

Moving on to the direct tissue samples, Day 1 showed that the untreated group again had the highest levels of MMP – 9 and Sn PP had the smallest amount of MMP – 9. Day 3 presented the complete opposite: Sn PP with highest MMP – 9 and untreated with the lowest. Day 7 demonstrated that the tin PP group had the highest level of enzyme and the untreated and Co PP groups had very similar levels of MMP – 9. The untreated samples were highest on Day 1 and lowest on Day 3. The Co PP group levels were highest on Day 1 and lowest on Day 7. Lastly, the Co PP group levels were highest on Day 7 and lowest on Day 1.

Interspace tissue samples showed lower levels of MMP – 9 in general compared with skin and direct tissues. Day 1 groups had very similar levels of enzyme with the Sn PP group highest and untreated animals with the lowest levels. The same trend appeared for Day 3 that was seen in Day 1. Day 7 portrayed different results. The Sn PP treated samples had the highest levels of MMP – 9 and the Co PP group had the lowest. The untreated group, Co PP treated group, and Sn PP treated group were all highest on Day 3 and lowest on Day 7. See Figure 16. Statistical analysis was acheived using the program, SigmaStat. An ANOVA (Tukeys) test was performed. See Table 6.

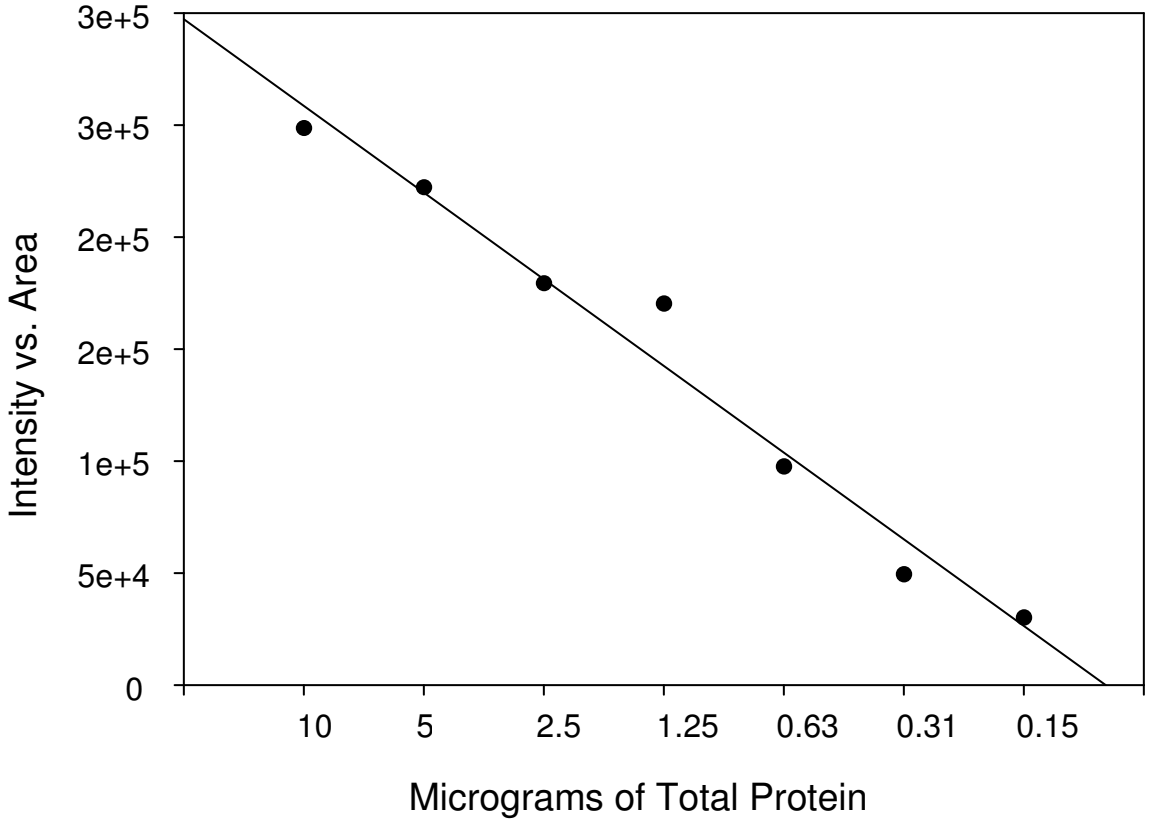

Figure 15: Linear Relationship Between Matrix Metalloproteinase-9 Levels and Densitometry. Serial 2-fold dilutions of a single sample were subjected to gelatin zymography. This is a log vs. log plot. Results indicate that the zones of clearing have linear dependency with MMP-9 concentration.

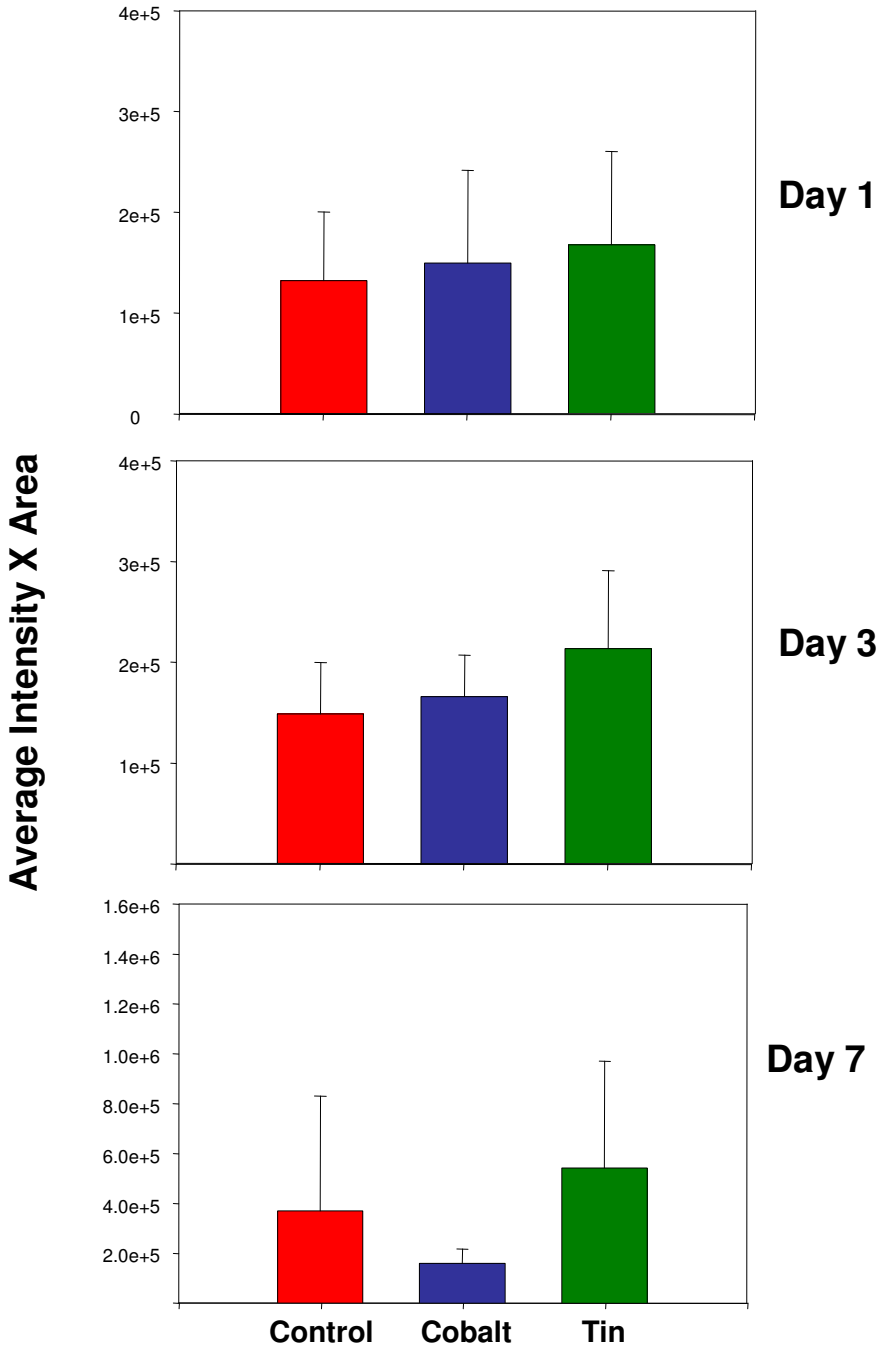

Figure 16: Gelatin Zymography of Interspace Tissues

Table 6: Statistical Analysis (ANOVA) for Gelatin Zymography Interspace Tissues

One Way Analysis of Variance Thursday, December 11, 2008, 18:02:10

Data source: Data 1 in Notebook

Normality Test: Failed (P = 0.024)

Test execution ended by user request, ANOVA on Ranks begun

Kruskal-Wallis One Way Analysis of Variance on Ranks Thursday, December 11, 2008, 18:02:10

Data source: Data 1 in Notebook

Group	**N**	**Missing**
Control Day 1	8	0
Cobalt Day 1	8	0
Tin Day 1	7	0
Control Day 3	7	0
Cobalt Day 3	7	0
Tin Day 3	7	0
Control Day 7	7	0
Cobalt Day 7	7	0
Tin Day 7	6	0

Group	**Median**	**25%**	**75%**
Control Day 1	181798.500	122575.000	257089.000
Cobalt Day 1	201503.500	132543.500	284487.500
Tin Day 1	232309.000	137981.000	301698.000
Control Day 3	181456.000	137962.500	268782.750
Cobalt Day 3	160583.000	92673.250	216154.750
Tin Day 3	236226.000	180620.000	249004.000
Control Day 7	276065.000	157940.250	328486.000
Cobalt Day 7	185773.000	161727.750	268342.500
Tin Day 7	372996.500	181368.000	584495.000

H = 8.673 with 8 degrees of freedom. (P = 0.371)

The differences in the median values among the treatment groups are not great enough to exclude the possibility that the difference is due to random sampling variability; there is not a statistically significant difference (P = 0.371)

Collagenase Assay

Collagenase is an enzyme that cleaves collagen into two fragments. At certain temperatures, the two fragments formed will denature. The radioactive collagen type I used will fluoresce to detect activity.

The tissue samples used in these assays did not show any cleavage of collagen. The wound fluid was used in every assay as a common standard. This wound fluid would show the two fragments of collagen on each assay, and the hope was to see these fragments in certain tissues. The reason these fragments did not show up is unknown. The tissues may have been sitting for too long since this was the last test performed, but it is hard to tell. Neither treatment options nor days of harvest made a difference in the tissue samples pertaining to the collagenase assay. By observing figures 17-19, the only fragments observed on the all assays were the wound fluid samples.

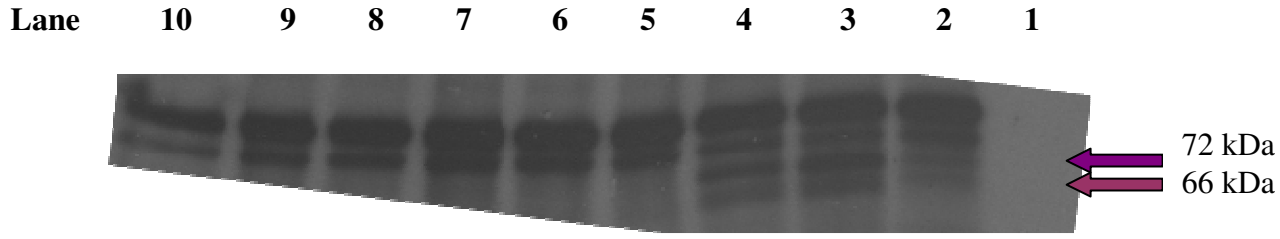

Lane 1: Marker

Lane 2: Wound Fluid Negative

Lane 3: Wound Fluid Active

Lane 4: Wound Fluid Total

Lane 5: 0910 Interspace Control Day 1 Active

Lane 6: 0910 Interspace Control Day 1 Total

Lane 7: 0502 Interspace Cobalt PP Day 1 Active

Lane 8: 0502 Interspace Cobalt PP Day 1 Total

Lane 9: 0803 Interspace Tin PP Day 1 Active

Lane 10: 0803 Interspace Tin PP Day 1 Total

Figure 17 : Collagenase Activity Assay 1

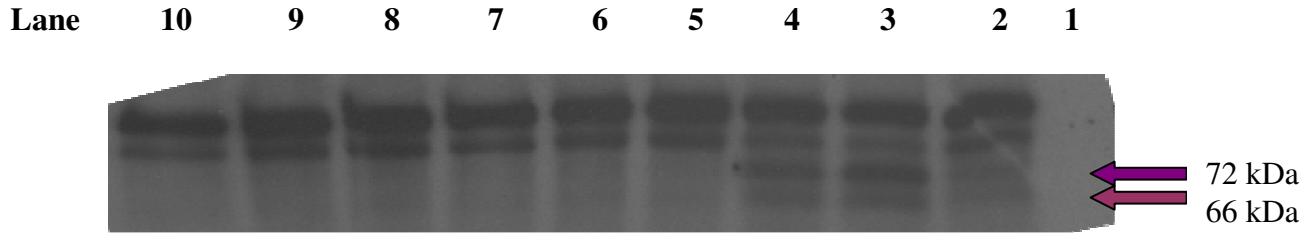

Lane 1: Marker

Lane 2: Wound Fluid Negative

Lane 3: Wound Fluid Active

Lane 4: Wound Fluid Total

Lane 5: 0306 Interspace Control Day 3 Active

Lane 6: 0306 Interspace Control Day 3 Total

Lane 7: 0406 Interspace Cobalt PP Day 3 Active

Lane 8: 0406 Interspace Cobalt PP Day 3 Total

Lane 9: 0903 Interspace Tin PP Day 3 Active

Lane 10: 0903 Interspace Tin PP Day 3 Total

Figure 18: Collagenase Activity Assay 2

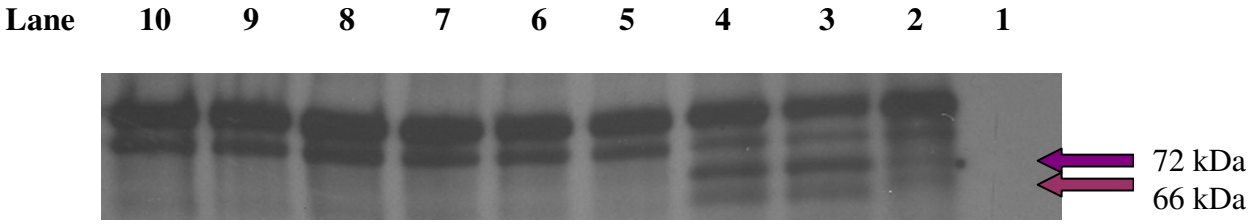

Lane 1: Marker

Lane 2: Wound Fluid Negative

Lane 3: Wound Fluid Active

Lane 4: Wound Fluid Total

Lane 5: 0609 Interspace Control Day 7 Active

Lane 6: 0609 Interspace Control Day 7 Total

Lane 7: 0408 Interspace Cobalt PP Day 7 Active

Lane 8: 0408 Interspace Cobalt PP Day 7 Total

Lane 9: 0901 Interspace Tin PP Day 7 Active

Lane 10: 0901 Interspace Tin PP Day 7 Total

Figure 19: Collagenase Activity Assay 3

Discussion

Burn wound conversion is an ongoing struggle for physicians and their burn patients. Research is being conducted in order to try and understand the mechanics of burn conversion and methods that can help to prevent it. This study examined the ability of two heavy metal protoporphyrins to modulate burn wound conversion in an animal model. Heavy metal protoporphyrins are modulators of the expression or activity of HO-1. Both Co PP and Sn PP induced the expression of HO-1 at the protein level. Sn PP is also an effective inhibitor of HO-1 activity. Animals receiving a single bolus of Co PP 24 hrs prior to burn injury exhibited significantly less necrosis than either of the other two groups.

In general, levels of inflammation within the interspace region as reflected by MPO activity and MMP-9 zymography correlated with levels of necrosis. Attempts at assessing collagenolytic activity were not successful. Neutrophil collagenase (MMP-8) is abundant in human neutrophils and wound fluid obtained from a human chronic wound contained easily detectable levels collagenolytic activity.

This research model was conducted using rats. The downside to this is that factors tested in rats cannot be directly compared to humans. For example, when the collagenase assay was performed, MMP-8 was abundant in human wound fluid, but not in the animal tissue. A possibility could be that MMP-8 is just not involved in inflammation in rats as it is in humans. The data collected appeared to correlate with research pertaining to humans, but it can not be certain. Until more research is

conducted in human burn tissue, it is hard to determine whether this model can be translated to humans.

An additional issue is whether heavy metal protoporphyrins can still significantly modulate conversion when administered post-wounding. One of the disadvantages to burn research is that it is impossible to know when an individual will be burned. An interesting experiment would be to determine if heavy metal protoporphyrins have any effect when administered to rats after the injury has occurred. This could allow for a more practical method reducing burn wound conversion.

Although heavy metal protopophyrins modulate HO-1 expression and activity, the approach used in this study does not definitively address whether HO-1 expression itself, has a role in modulation of conversion. Future studies directly testing the ability of HO-1 to modulate burn wound conversion still need to be performed. If HO-1 is indeed serving a function, it will be necessary to determine the mechanism involved. It has not been determined where exactly HO-1 acting. Is HO-1 mainly removing heme, which can act as a potent oxidant? The key purpose of HO-1 may be to induce carbon monoxide (CO) and biliverdin/bilirubin, which act as anti-oxidants and anti-apoptotic molecules. Focusing on the true manner in which HO-1 expression occurs could give extremely effective results. Lastly, it would be beneficial to determine how CO and biliverdin/bilirubin directly or indirectly influence the injury. Their specific targets of action would help to ascertain methods involved in decreasing the inflammatory response in burn wounds in order to prevent conversion.

Literature Cited

Literature Cited

Anderson, K. E., Simionatto, C. S., Drummond, G. S., & Kappas, A. (1984). Tissue distribution and disposition of tin-protoporphyrin, a potent competitive inhibitor of heme oxygenase. *American Society for Pharmacology and Experimental Therapeutics, 228*(2), 327-333.

Barrick, B., Edward J. Campbell, M.D., & Caroline A. Owen, M.D., Ph.D. (1999). Leukocyte proteinases in wound healing: Roles in physiologic and pathologic processes. *Wound Repair and Regeneration, 7. No. 6* (November-December), 410-422.

Barton, R. M., Kokoska, E. R., Wainwright, D. J., & Parks, D. H. (2006). Pathophysiology of thermal injury. In T. A. Miller (Ed.), *Modern surgical care* (3rd Edition ed., pp. 1085-1102). USA: Informa Healthcare.

Basadre, J. O., Sugi, K., Traber, D. L., Traber, L. D., Niehaus, G. D., & Herndon, D. N. (1988). The effect of leukocyte depletion on smoke inhalation injury in sheep. *Surgery, 104*(2), 208-215.

Benson, A., Dickson, W. A., & Boyce, D. E. (2006). ABC of wound healing: Burns. *BMJ, 332*, November 4, 2008.

Brannon, H. (2007). *Skin anatomy.* Retrieved November 18, 2008, from dermatology.about.com/cs/skinanatomy/a/anatomy

Breslow, E., Chandra, R., & Kappas, A. (1986). Biochemical properties of the heme oxygenase inhibitor, sn - protoporphyrin. *The Journal of Biological Chemistry, 261. No. 7* (March), 3136-3141.

Broughton, G. I., Jeffrey E. Janis, M.D., & Christopher E. Attinger, M.D. (2006). The basic science of wound healing. *Plastic and Reconstructive Surgery, 117, Number 7S* (June Supplement), 12S-34S.

Broughton, G. I., Jeffrey E. Janis, M.D., & Christopher E. Attinger, M.D. (2006). A brief history of wound care. *Plastic and Reconstructive Surgery, 117, Number 7S* (June Supplement), 6S-11S.

Broughton, G. I., Jeffrey E. Janis, M.D., & Christopher E. Attinger, M.D. (2006). Wound healing: An overview. *Plastic and Reconstructive Surgery, 117, Number 7S* (June Supplement), 1e-S-32e-S.

Burger, D., Xiang, F., Hammoud, L., Lu, X., & Feng, Q. (2008). Role of heme oxygenase-1 in the cardioprotective effects of erythropoietin during myocardial ischemia and reperfusion. *American Journal of Physiology - Heart and Circulatory Physiology,*1-39.

Cain, B. S., Harken, A. H., & Meldrum, D. R. (1999). Therapeutic strategies to reduce TNF-alpha mediated cardiac contractile depression following ischemia and reperfusion. *Journal of Molecular Cell Cardiology, 31*(5), 931-947.

Cynober, L., Desmoulins, D., Lioret, N., Aussel, C., Hirsch-Marie, H., & Saizy, R. (1985). Significance of vitamin A and retinol binding protein serum levels after burn injury. *International Journal of Clinical Chemistry, 148*(3), 247-253.

Darling, D. (1999). *Hypodermis.* Retrieved November 18, 2008, from www.daviddarling.info/encyclopedia/H/hypodermis

Demling, R., & LaLonde, C. (1990). Early postburn lipid peroxidation: Effect of ibuprofen and allopurinol. *Surgery, 107*(1), 85-93.

Demling, R., & LaLonde, C. (1990). Identification and modifications of the pulmonary and systemic inflammatory and biochemical changes caused by a skin burn. *Journal of Trauma, 30*(12), S57-S62.

Demling, R., LaLonde, C., Ikegami, K., Picard, L., & Nayak, U. (1995). Alpha-tocopherol attenuates lung edema and lipid peroxidation caused by acute zymosan-induced peritonitis. *Surgery, 117*(2), 226-231.

Devey, L., Ferenbach, D., Mohr, E., Sangster, K., Bellamy, C. O., Hughes, J., et al. (2008). Tissue-resident macrophages protect the liver from ischemia reperfusion injury via a heme oxygenase-1-dependent mechanism. *Molecular Therapy,* 1-8.

Devgan, L., Satyanarayan Bhat, P. D., S. Aylward, B. A., & Robert J. Spence, M.D. (2006). Modalities for the assessment of burn wound depth. *Journal of Burns and Wounds, 5*(2), 1-3.

Dokumcu, Z., Ergun, O., Celik, H. A., Aydemir, S., Sezak, M., Ozok, G., et al. (2008). Clostridial collagenase aggrevates the systemic inflammatory response in rats with partial-thickness burns. *Burns, 34*(7), 935-941.

Ehrlich, H. P., & Regas, F. C. (1992). Elucidating the vascular response to burns with a new rat model. *Journal of Trauma, 32*(5), 557-563.

Farombi, E. O., & Surh, Y. (2006). Heme oxygenase - 1 as a potential therapeutic target for hepatoprotection. *Journal of Biochemistry and Molecular Biology, 39. No. 5* (September), 479-491.

Gary, J. (2008). *The 3 skin layers: Epidermis, dermis, subcutaneous fat.* Retrieved Novermber 18, 2008, from www.pg.com/science/skincare/Skin_tws_10

Giroir, B. P., Horton, J. W., White, D. J., McIntyre, K. L., & Lin, C. Q. (1994). Inhibition of tumor necrosis factor prevents myocardial dysfunction during burn shock. *American Journal of Physiology, 267*(1 Pt 2), H118-H124.

Gomez, R., & Leopoldo C. Cancio, M.D. (2007). Management of burn wounds in the emergency department. *Emergency Medicine Clinics of North America, 25*, 135-146.

Goodis, J. (2008). Burns, thermal. *EMedicine from WebMD,* November 3, 2008.

Hettiaratchy, S., & Dziewulski, P. (2004). ABC of burns: Pathophysiology and types of burns. *BMJ - PubMed Central, 328*(7453), November 3, 2008.

Horton, J., Garcia, N., White, D., & Keffer, J. (1995). Post burn cardiac contractile function and biochemical markers of post burn cardiac injury. *Journal of the Am. Coll. Surg., 181*, 289-298.

Horton, J. W. (1996). Cellular basis for burn-mediated cardiac dysfunction in adult rabbits. *American Journal of Physiology, 271*(6 Pt 2), H2615-H2621.

Horton, J. W. (2003). Free radicals and lipid peroxidation mediated injury in burn trauma: The role of antioxidant therapy. *Toxicology, 189*(1-2), 75-88.

Isik, S., Sahin, U., Ilgan, S., Guler, M., Gunalp, B., & Selmanpakoglu, N. (1998). Saving the zone of stasis in burns with recombinant tissue-type plasminogen activator (r-tPA): An experimental study in rats. *Burns, 24*(October), 217-223.

Juan, S. H., Lee, T. S., Tseng, K. W., Liou, J. Y., Shyue, S. K., Wu, K. K., et al. (2001). Adenovirus-mediated heme oxygenase-1 gene transfer inhibits the development of atherosclerosis in apolipoprotein E-deficient mice. *Circulation, 104*, 1519-1525.

Kappas, A., & Drummond, G. S. (1986). Control of heme metabolism with synthetic metalloporphyrins. *American Society for Clinical Investigation, Inc., 77* (February), 335-339.

Kenet, Barney J. M.D., & Lawler, P. (1994). The structure and function of human skin. *Saving your skin* (http://www.healtheez.com/hypodermis.htm ed., pp. 24-26). United States: Four Walls Eight Windows.

Kulina, R. (2008). Induction of heme oxygenase by a carbon monoxide releasing molecule. (Master of Science, Virginia Commonwealth University). *VCU Digital Archives, Physiology Department*

LaLonde, C., Nayak, U., Hennigan, J., & Demling, R. (1997). Excessive liver oxidant stress causes mortality in response to burn injury combined with endotoxin and is prevented with antioxidants. *Journal of Burn Care Rehabilitation, 18*(3), 187-192.

LaLonde, C., Nayak, U., Hennigan, J., & Demling, R. (1997). Plasma catalase and glutathione levels are decreased in response to inhalation injury. *Journal of Burn Care Rehabilitation, 18*(6), 515-519.

LaLonde, C., Youn, Y. K., & Demling, R. (1992). Oxidants and the pathophysiology of burn and smoke inhalation injury. *Free Radical Biological Medicine, 12*(5), 409-415.

Laskey, R. A. (2003). *Review 23: Efficient detection of biomolecules by autoradiography, fluorography, or chemiluminescence.* Retrieved November 23, 2008, from www.amershambiosciences.com/aptrix/upp00919.nsf/(FileDownload)?OpenAgent&docid=1DC784945E4EABB3C1256BB26000DB&file=review23_part1.pdf

Latha, B., & Babu, M. (2001). The involvement of free radicals in burn injury: A review. *Burns, 27*, 309-317.

Lau, D., Mollnau, H., Eiserich, J. P., Freeman, B. A., Daiber, A., Gehling, U. M., et al. (2004). Myeloperoxidase mediates neutrophil activation by association with CD11b/CD18 integrins. *Proc. Natl. Acad. Sci. USA, 102*(2), 431-436.

Leikin, J. B., & Martin S. Lipsky, M.D. (2003). Skin. *Complete medical encyclopedia* (American Medical Association ed., pp. 1126-1127). New York, United States: Random House.

Mahajan, A. L., Tenorio, X., Pepper, M. S., Baetens, D., Montandon, D., Schlaudraff, K., et al. (2006). Progressive tissue injury in burns is reduced by rNAPc2. *Burns, 32* (February), 957-963.

Mathy-Hartert, M., Bourgeois, E., Grulke, S., Deby-Dupont, G., Caudron, I., Deby, C., et al. (1998). Purification of myeloperoxidase equine polymorphonuclear leucocytes. *Canadian Journal of Veterinary Medicine, 62*(2), 127-132.

McCord, J. M., & Fridovich, I. (1968). The reduction of cytochrome c by milk xanthine oxidase. *Journal of Biology and Chemistry, 243*

Mileski, W. J., Winn, R. K., Harlan, J. M., & Rice, C. L. (1991). Transient inhibition of neutrophil adherence with the anti-CD18 monoclonal antibody 60.3 does not increase mortality rates in abdominal sepsis. *Surgery, 109*(4), 497-501.

Minamino, T., Christou, H., Hsieh, C. M., Liu, Y., Dhawan, V., Abraham, N. G., et al. (2001). Targeted expression of heme oxygenase-1 prevents the pulmonary inflammatory and vascular responses to hypoxia. *Proc. Natl. Acad. Sci. U. S. A, 98*, 8798-8803.

Mustoe, T. A., Kristina O'Shaughnessy, M. D., & Oliver Kloeters, M. D. (2006). Chronic wound pathogenesis and current treatment strategies: A unifying hypothesis. *Plastic and Reconstructive Surgery, 117, Number 7S* (June Supplement), 35S-41S.

Nguyen, T. T., Cox, C. S., Traber, D. L., Gasser, H., Redl, H., Schlag, G., et al. (1993). Free radical activity and loss of plasma antioxidants, vitamin E, and sulfhydryl groups in patients with burns. *Journal of Burn Care Rehabilitation, 14*(6), 602-609.

Niimi, M., Takashina, M., Takami, H., Ikeda, Y., Shatari, T., Hamano, K., et al. (2000). Overexpression of heme oxygenase-1 protects allogeneic thyroid grafts from rejection in naive mice. *Surgery, 128*, 910-917.

Parihar, A., Parihar, M. J., Milner, S., & Bhat, S. (2007). Oxidative stress and anti-oxidative mobilization in burn injury. *Burns, (*April), 1-12.

Pharmacorama Drug Knowledge. (2008). *Bradykinin.* Retrieved November 18, 2008, from www.pharmacorama.com/en/Sections/Angiotensin_2

Poss, K. D., & Tonegawa, S. (1997). Heme oxygenase-1 is required for mammalian iron reutilization. *Proc. Natl. Acad. Sci. USA, 94* (September), 10919-10924.

Rai, K., & Courtemanche, A. D. (1975). Vitamin A assay in burned patients. *Journal of Trauma, 15*(5), 419-424.

Rawlingson, A. (2003). Nitric oxide, inflammation and acute burn injury. *Burns, 29*(7), 631-640.

Robson, M. C. (1979). An easy access incision for the removal of some intraoral malignant tumors. *Journal of Plastic and Reconstructive Surgery, 64*(6), 834-835.

Ryter, S., W., Alam, J., & Choi, Augustine M. K. (2006). Heme oxygenase - 1/Carbon monoxide: From basic science to therapeutic applications. *Physiological Review, 86* (April), 583-650.

Sardana, M. K., & Kappas, A. (1987). Dual control mechanism for heme oxygenase: Tin (IV)-protoporphryin potently inhibits enzyme activity while markedly increasing content of enzyme protein in liver. *Proc. National Academy of Science, 84* (April), 2464-2468.

Sasaki, T. (1990). Studies on oxygen derived free radicals in acute pancreatic damage in rats -- pancreatic damage experimentally induced diethyldithiocarbamate. *Nippon Shokakibyo Gakkai Zasshi, 87*(6), 1436-1443.

Serhan, C. N., Brain, S. D., Buckley, C. D., Gilroy, D. W., Haslett, C., O'Neill, L. A. J., et al. (2007). Resolution of inflammation: State of the art, definitions and terms. *The FASEB Journal, 21* (February), 325-327.

Singh, V., Devgan, L., Bhat, S., & Milner, S. M. (2007). The pathogenesis of burn wound conversion. *Annals of Plastic Surgery, 59. No. 1* (July), 109-115.

Sun, B., Jin, Q., Sun, Y., Sun, Z., Chen, X., Chen, Z., et al. (2007). Carbon liberated from CO-releasing molecules attenuates leukocyte infiltration in the small intestine of thermally injured mice. *World Journal of Gastroenterology, 13. No. 46* (December), 6183-6190.

Taille, C., Foresti, R., Lanone, S., Zedda, C., Green, C., Aubier, M., et al. (2001). Protective role of heme oxygenases against endotoxin-induced diaphragmatic dysfunction in rats. *American Journal of Respiratory Critical Care Medicine, 163*, 753-761.

Tracz, M. J., Juncos, J. P., Grande, J. P., Croatt, A. J., Ackerman, A. W., Katusic, Z. S., et al. (2008). Induction of heme oxygenase-1 is a beneficial response in a murine model of venous thrombosis. *The American Journal of Pathology, 173*, 1882-1890.

Tyler, M. P. H., Watts, A. M. I., Perry, M. E., Roberts, A. H. N., & McGrouther, A. D. (2001). Dermal cellular inflammation in burns: An insight into the function of dermal microvascular anatomy. *Burns, 27*(5), 433-438.

Wanek, S., & Wolf, S. E. (2007). Metabolic response to injury and role of anabolic hormones. *Lippincott Williams & Wilkins,* , 272-277.

Warden, G. D., & Heimbach, D. M. (1999). Burns. *Principals of surgery* (7th Edition ed., pp. 223-262). New York, United States: Schwartz SI.

Waterborg, j. H., & Matthews, H. R. (1994). Fluorography of polyacrylamide gels containing tritium. In J. M. Walker (Ed.), *Basic protein and peptide protocols* (v 32 ed., pp. 163-167). Totowa, New Jersey: Humana Press.

Weeks, B. S., & Xu, R. X. (2004). Brief introduction to the history of burns medical science. In X. Sun (Ed.), *Burns regenerative medicine and therapy* (pp. 1-3)

Yachie, A., Niida, Y., Wada, T., Igarashi, N., Kaneda, H., Toma, T., et al. (1999). Oxidative stress causes enhanced endothelial cell injury in human heme oxygenase-1 deficiency. *Journal of Clinical Investigation, 103*(1), 129-135.

Yager, D. R., & Nwomeh, B. C. (1999). The proteolytic environment of chronic wounds. *Wound Repair and Regeneration, 7. No. 6* (November-December), 433-441.

Yager, D. R., Zhang, L., Liang, H., Diegelmann, R. F., & Cohen, I. K. (1996). Wound fluids from human pressure ulcers contain elevated matrix metalloproteinase levels and activity compared to surgical wound fluids. *The Journal of Investigative Dermatology, 107. No. 9* (November), 743-748.

VITA

Katie Lynne Braun was born in Reading, Pennsylvania on June 24, 1984. She grew up all over the United States and also overseas in Ukraine and Turkey. In June 2002 she graduated from George C. Marshall High School in Ankara, Turkey. James Madison University in Harrisonburg, Virginia was the next step of her journey. She graduated with a Bachelor of Science in Health Science in August of 2006. She then decided to enroll in the Physiology Certificate program at Virginia Commonwealth University graduate school in Richmond, Virginia. After completing the certificate program, she transferred over to the Master of Science degree track in the Department of Physiology. Research was conducted in the Department of Surgery from 2007 – 2008. While doing research, she also worked part time, volunteered as a recreational therapy assistant at the Children's Hospital of Richmond, and succeeded as a TA in an undergraduate physiology course at Virginia Commonwealth University. She worked full time as a lifeguard in the summer of 2008, while still working on her degree. At the end of the fall semester 2008, she completed her Master of Science degree in Physiology. She is currently applying to medical schools and nursing programs for the fall of 2009.